

Regulation of retinal interneuron subtype identity by the *Iroquois* homeobox gene *Irx6*

Erin N. Star^{1,*}, Minyan Zhu^{1,*}, Zhiwei Shi¹, Haiquan Liu¹, Mohammad Pashmfroush², Yves Sauve³, Benoit G. Bruneau⁴ and Robert L. Chow^{1,‡}

SUMMARY

Interneuronal subtype diversity lies at the heart of the distinct molecular properties and synaptic connections that shape the formation of the neuronal circuits that are necessary for the complex spatial and temporal processing of sensory information. Here, we investigate the role of *Irx6*, a member of the *Iroquois* homeodomain transcription factor family, in regulating the development of retinal bipolar interneurons. Using a knock-in reporter approach, we show that, in the mouse retina, *Irx6* is expressed in type 2 and 3a OFF bipolar interneurons and is required for the expression of cell type-specific markers in these cells, likely through direct transcriptional regulation. In *Irx6* mutant mice, presumptive type 3a bipolar cells exhibit an expansion of their axonal projection domain to the entire OFF region of the inner plexiform layer, and adopt molecular features of both type 2 and 3a bipolar cells, highlighted by the ectopic upregulation of neurokinin 3 receptor (Nk3r) and *Vsx1*. These findings reveal *Irx6* as a key regulator of type 3a bipolar cell identity that prevents these cells from adopting characteristic features of type 2 bipolar cells. Analysis of the *Irx6;Vsx1* double null retina suggests that the terminal differentiation of type 2 bipolar cells is dependent on the combined expression of the transcription factors *Irx6* and *Vsx1*, but also points to the existence of *Irx6;Vsx1*-independent mechanisms in regulating OFF bipolar subtype-specific gene expression. This work provides insight into the generation of neuronal subtypes by revealing a mechanism in which opposing, yet interdependent, transcription factors regulate subtype identity.

KEY WORDS: Retina, Transcription factor, Bipolar interneuron, Cell type diversity, Mouse

INTRODUCTION

The simple organization of the retina into five major neuronal classes makes it an excellent model for studying the developmental mechanisms that underlie cell type diversity (Ohsawa and Kageyama, 2008). The simple neuronal cell class organization of the retina, however, is accompanied by high degree of cell type heterogeneity. In mammals, the five major retinal neuronal classes give rise to 55 morphological cell types (Masland, 2001), which comprise functionally diverse circuits within the retina (Gollisch and Meister, 2010). The current literature defines 11 bipolar cell types based on morphology, gene expression and axonal tiling properties (Wässle et al., 2009) (see Fig. 1).

Combinatorial transcription factor coding based on the differential expression of homeodomain and basic helix-loop-helix transcription factors has been identified as a common mechanism underlying neuronal cell type diversity (Fode et al., 2000; Guillemot, 2007; Ma, 2006; Ohsawa and Kageyama, 2008; Shirasaki and Pfaff, 2002). Several homeodomain and basic helix-loop-helix transcription factors are important for the development and homeostasis of distinct retinal bipolar cell subtypes. The development of type 2 and 3 OFF bipolar cells is regulated by the overlapping requirements of several transcription factors (Cheng et

al., 2005; Chow et al., 2004; Feng et al., 2006; Kerschensteiner et al., 2008; Ohtoshi et al., 2004). In mice lacking *Vsx1* or *Irx5* homeobox gene function, type 2 and 3 bipolar cells are specified but have defects in their terminal differentiation marked by reduced expression of type 2 and 3 cell-specific markers (Chow et al., 2004; Ohtoshi et al., 2004; Shi et al., 2012; Cheng et al., 2005). In *Vsx1*-mutant mice, expression of the type 2 cell markers recoverin (Rcvrn), neurokinin 3 receptor (Nk3r; Tacr3 – Mouse Genome Informatics) and *Neto1* is reduced (Chow et al., 2004; Ohtoshi et al., 2004), type 3 cells have reduced *Cabp5* immunolabeling in the axon terminal region (Chow et al., 2004), and there is a reduction in the total number of Hcn4-positive type 3a bipolar cells (Shi et al., 2012). In *Irx5* mutants, type 2 bipolar cells have reduced levels of recoverin immunolabeling, but normal levels of Nk3r immunolabeling, and type 3 cells exhibit reduced levels of *Cabp5* within their axon terminals (Cheng et al., 2005). Mice lacking the basic helix-loop-helix transcription factor *Bhlhb5* (*Bhlhb22* – Mouse Genome Informatics) have a reduction of recoverin and Nk3r immunolabeled type 2 cells, and also have a reduction in the total number of *Vsx1*-labeled bipolar cells (Feng et al., 2006). Although *Vsx1* is not necessary for *Irx5* bipolar cell expression (Cheng et al., 2005), it negatively regulates its own expression (Chow et al., 2004) and is a positive regulator of *Bhlhb5* (M.Z. and R.L.C., unpublished). Conversely, *Bhlhb5* functions as a positive regulator of *Vsx1* in putative type 2 cells (Feng et al., 2006).

In the present study, we investigate the role of the *Iroquois* family member *Irx6* in retinal development. The *Iroquois* (*Irx*) gene family encodes transcription factors that harbor a 63 amino acid TALE family homeodomain and a 9 amino acid conserved motif outside of the homeodomain known as the *Iro* box (Bilioni et al., 2005). Mammals have six *Irx* genes that exist in two clusters: the *IrxA* cluster (*Irx1*, *Irx2* and *Irx4*) and *IrxB* cluster (*Irx3*, *Irx5* and *Irx6*) (Gómez-Skarmeta and Modolell, 2002). Studies in both

¹Department of Biology, University of Victoria, Victoria, BC V8W 3N5, Canada.

²Broad Center for Regenerative Medicine and Stem Cell Research, Division of Cardiovascular Medicine and University of Southern California, 2250 Alcazar Street CSC240, Los Angeles, CA 90033, USA. ³Department of Ophthalmology, University of Alberta, Edmonton, AB T5H 3V9. ⁴Gladstone Institute of Cardiovascular Disease, University of California – San Francisco, 1650 Owens Street, San Francisco, CA 94158, USA.

*These authors contributed equally to this work

‡Author for correspondence (bobchow@uvic.ca)

Drosophila and vertebrate models have implicated Iroquois genes in axon targeting events (Grillenconi et al., 1998; Jin et al., 2003; Sato et al., 2006).

We show that *Irx6* is expressed in type 2 and 3a bipolar cells where it is required for the expression of cell type-specific markers, including *Bhlhb5*. Presumptive type 3a cells in the *Irx6* mutant stratify correctly to the OFF sublamina of the inner plexiform layer, but instead of the normal restricted segregation of their axon termini to sublamina 2, they can stratify within both OFF sublamina 1 and 2. Furthermore, these cells adopt molecular features of both type 2 and 3a cells, highlighted by the ectopic expression of *Vsx1* and *Nk3r*. These defects in type 3a cell development in the *Irx6* mutant appear to be independent of *Vsx1* function. Our findings reveal *Irx6* as a core regulator of type 3a bipolar cell identity that prevents them from adopting features characteristic of type 2 bipolar cells, and suggest that terminal differentiation of type 2 bipolar cells is dependent on the combined activity of *Vsx1* and *Irx6*.

MATERIALS AND METHODS

Generation of *Irx6^{lacZ}* knock-in mice

Gene targeting was performed in R1 (Svj129) embryonic stem (ES) cells. The targeting construct was generated by screening an M13 mouse R1 genomic library (Stratagene) with probes for *Irx6* (supplementary material Fig. S1). Chimeric mice were generated by blastocyst injection of homologous recombinant ES cells (Scripps Research Institute Transgenic Core Facility), and the resulting mice were bred with the 129S1/SvImJ mouse strain (Jackson Laboratory). All experiments on mice were conducted with the approval of the University of Victoria Animal Care Committee.

Immunohistochemistry and microscopy

Unless otherwise noted, all retinas were taken from 2- to 3-month-old mice, and central sections of the retina were used for imaging. Eyes were fixed in 4% paraformaldehyde in PBS for 1 hour (on ice) or for 20 minutes (room temperature), cryoprotected in 30% sucrose, embedded in Tissue-Tek OCT (Sakura Finetek), and cryosectioned at 14 μ m. Primary antibody information is given in supplementary material Table S1. Secondary antibodies were conjugated to Alexa dyes (Invitrogen) or Cy3 (anti-guinea pig; Jackson ImmunoResearch). DraQ5 (Alexis Biochemicals) was used for nuclear labeling. For detection of β -galactosidase activity, sections were incubated in 1 mg/ml bromo-chloro-indolyl-galactopyranoside (X-gal) overnight at 37°C, as previously described (Mombaerts et al., 1996). Images were taken on a confocal microscope (Nikon Eclipse TE2000-U C1) and processed using Adobe Photoshop CS3. Cell counting and measurement of the fluorescence intensity within a 100 \times 10 μ m region of interest was carried out using EZ-C1 Version 3.60 software (Nikon Instruments). Data are presented as mean \pm s.e.m. Statistical analysis was performed using Student's *t*-test.

PCR genotyping

The genomic DNA was prepared from mice ear clips. The following primers were used for *Irx6* genotyping: IRX6-PF (GGCGCCTGCTCCT-GCAGCCC), IRX6-IR (GGATGTGCTGCCATACGGGTGT) and LacZR (AGATGAAACGCCGAGTTAACGC). The *Vsx1* mutant mouse (AltB5 or Δ 1-4 line) has been previously described (Chow et al., 2004).

Luciferase assay

HEK cells were transfected and assayed 24 hours later for luciferase activity with Dual-Glo luciferase assay system (Promega) according to the manufacturer's protocol. Luciferase activity was measured by a Wallac 1420 Multilabel Counter (PerkinElmer). The vectors used in the assay are described in supplementary material Table S2.

Electroretinography

Retinal function of mice from four experimental groups (*Irx6^{lacZ}*; *Vsx1^{+/AltB5}*; *Vsx1^{AltB5/AltB5}*; *Irx6^{lacZ}* and *Irx6^{lacZ/lacZ}*) was studied

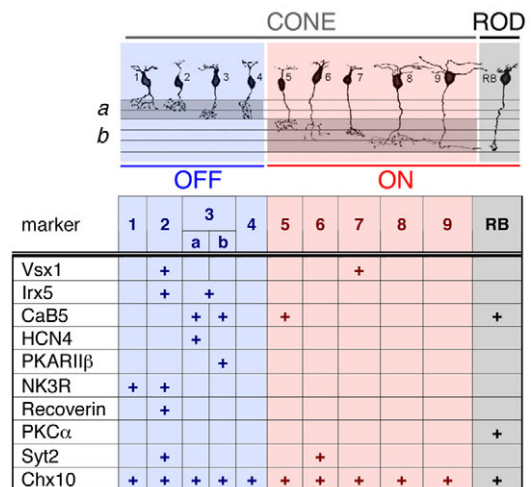


Fig. 1. Bipolar cell type-specific markers used in this study.

Morphological cell types [adapted with permission from Ghosh et al. (Ghosh et al., 2004)]. Markers used are: *Vsx1* (Chow et al., 2001; Chow et al., 2004; Shi et al., 2011); *Irx5* (Cheng et al., 2005); *CaB5* (Haverkamp et al., 2003; Ghosh et al., 2004); *Hcn4* and *PKARIIβ* (Matargua et al 2007); *Nk3r* (Haverkamp et al., 2003; Ghosh et al., 2004); *recoverin* (Haverkamp et al., 2003); *PKCα* (Negishi et al., 1988; Haverkamp and Wässle, 2000); *Syt2* (Wässle, 2009); *Chx10* (Burmeister et al., 1996).

using the full field electroretinogram (ERG) as previously described (Alvarez et al., 2007). Light stimulation (10 μ second duration flashes), signal amplification (0.3-300 Hz bandpass) and data acquisition were provided by the Espion E² system (Diagnosys). Scotopic intensity responses consisted of single flash presentations at 19 increasing strengths from -5.22 to 2.86 log cds/m². Ten minutes after transition from dark to light (30 cd/m² white light background) adaptation, photopic intensity responses (30 cd/m² background light) were recorded at 11 increasing flash strengths ranging from -1.6 to 2.9 log cds/m², followed by OFF responses obtained with a square wave stimulus of 562.5 cd/m², lasting 800 mseconds.

RESULTS

Irx6 reporter expression in the developing and mature mouse retina

To investigate the role of *Irx6* in mouse retinal development, we generated a knock-in *lacZ* reporter allele (*Irx6^{lacZ}*) in which *Irx6* exon 1 and part of exon 2 was replaced by the *lacZ* gene (supplementary material Fig. S1). Whole-mount X-gal detection of the *lacZ* gene product, β -galactosidase in *Irx6^{lacZ}* mice at embryonic day 12.5 (E12.5) revealed scattered expression of the reporter throughout the embryo (Fig. 2B). X-gal staining was first detected in the central ganglion cell region of the retina in *Irx6^{lacZ}* mice beginning at embryonic day 13.5 (E13.5) (Fig. 2D). Owing to the lack of a suitable antibody, we were unable to confirm reporter expression using *Irx6* immunohistology. However, the onset and localization of the reporter expression is consistent with the previously described expression of *Irx6* mRNA in the retina (Cohen et al., 2000; Erkmann et al., 2000) (supplementary material Fig. S1), suggesting that the knock-in *lacZ* reporter faithfully recapitulates the normal *Irx6* expression pattern. By E16.5, there was strong expression of the *Irx6^{lacZ}* reporter in the developing retinal ganglion cell layer and optic nerve region (Fig. 2E). At postnatal day zero (P0), X-gal staining persisted in the ganglion cell layer, and was also observed in the apical margin region of the retina (Fig. 2G). By P7, reporter expression was detected in a

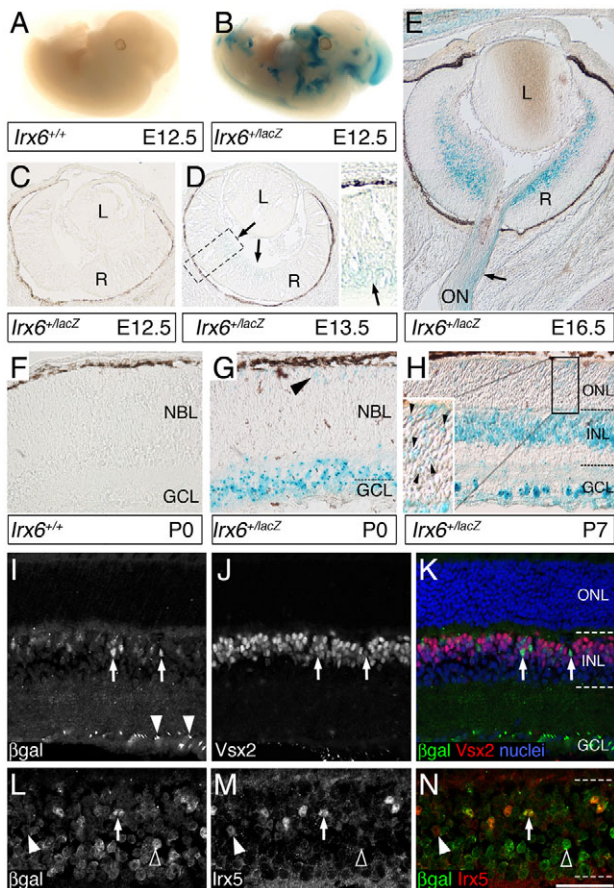


Fig. 2. Expression of the *Irx6*: β gal reporter during development of the mouse. (A-H) X-gal staining results. (A,B) E12.5 wild-type (A) and *Irx6*^{+/*lacZ*} (B) mouse, showing expression of *Irx6*: β gal in the midbrain. (C,D) Retinal section from an *Irx6*^{+/*lacZ*} mouse at E12.5 (C) and E13.5 (D); arrows in D indicate faint X-gal precipitate. (E) E16.5 retinal section from an *Irx6*^{+/*lacZ*} mouse showing staining down the optic nerve. (F-H) Wild type (F) and *Irx6*^{+/*lacZ*} (G,H) retina at P0 (F,G) and P7 (H), with arrowheads (G and H, inset) indicating staining in the newly formed ONL. (I,J) Immunohistochemistry of an *Irx6*^{+/*lacZ*} retina showing *Irx6*: β gal expression (I, arrows) and *Vsx2*/*Chx10* expression (J, arrows). Arrowheads in I indicate *Irx6*: β gal expression in the GCL. (K) Colocalization of *Irx6*: β gal and *Vsx2*/*Chx10* (arrows). The nuclear stain is Draq5. (L,M) *Irx6*: β gal (L, arrow) and *Irx5* (M, closed arrowhead) expression in the *Irx6*^{+/*lacZ*} retina. (N) An *Irx5*-positive, *Irx6*: β gal-negative cell (closed arrowhead); an *Irx5*-positive, *Irx6*: β gal-positive cell (arrow); and an *Irx5*-negative, *Irx6*: β gal-positive cell (open arrowhead). L, lens; R, retina; ON, optic nerve; NBL, neuroblast layer; GCL, ganglion cell layer; INL, inner nuclear layer; ONL, outer nuclear layer. Scale bar: 3 mm in A,B; 60 μ m in C,D; 100 μ m in E; 50 μ m in F-K; 25 μ m in L-N.

number of cells within the outer half of the inner nuclear layer and in the ganglion cell layer (Fig. 2H).

In the mature *Irx6*^{+/*lacZ*} retina, immunolabeling of the β -galactosidase reporter (*Irx6*: β gal) together with *Vsx2*/*Chx10*, a pan-bipolar transcription factor (Burmeister et al., 1996), indicated *Irx6* expression in a subset of bipolar cells (Fig. 2I-K). The *Irx6* homologue *Irx5*, was co-expressed in a subset of *Irx6*: β gal-immunolabeled bipolar cells (Fig. 2L-N). Not all *Irx5*-positive cells in the inner nuclear layer co-labeled with *Irx6*: β gal, and not all *Irx6*: β gal positive cells co-labeled with *Irx5* (Fig. 2L-N). Additionally, *Irx6*: β gal co-immunolabeled with a subset of cells

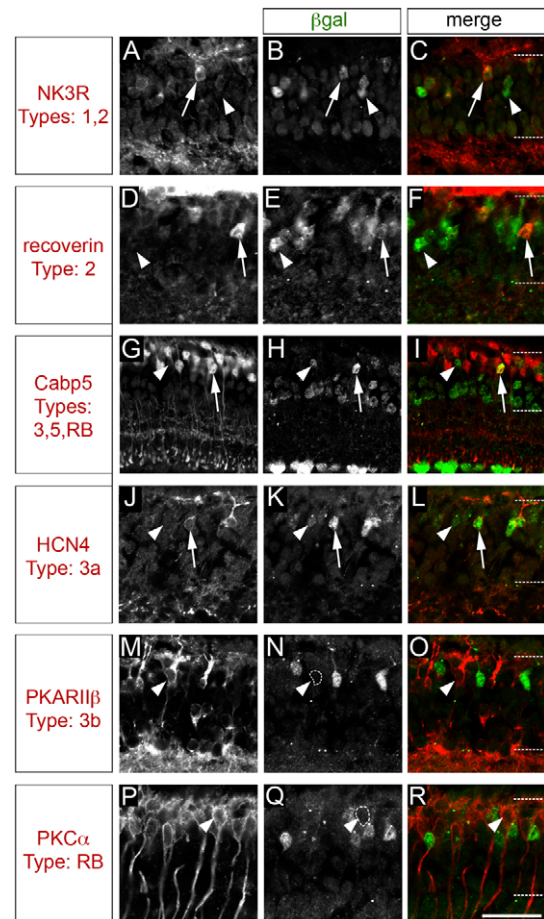


Fig. 3. The *Irx6*: β gal reporter is expressed in a subset of retinal bipolar cells. (A-F) In the mature *Irx6*^{+/*lacZ*} retina, the *Irx6*: β gal reporter is expressed in a subset of *Nk3r*- (A-C, arrow) and *recoverin*- (D-F, arrow) positive cells. (G-I) *Irx6*: β gal is also expressed in a subset of *Cabp5* cells (arrows). (J-L) *Irx6*: β gal colocalizes with the type 3a marker *Hcn4* (J-L, arrows), but not with the type 3b marker *PKAR1 β* (M-O). Arrowheads in A-O indicate β gal-labeled cells that are not co-labeled with the respective bipolar marker. (P-R) There is no colocalization between *PKC α* expression and *Irx6*: β gal expression. Arrowhead indicates a *PKC α* -positive cell that does not colabel with *Irx6*: β gal. Scale bar: 25 μ m.

expressing the ganglion cell marker *Brn3b* (*Pou4f2* – Mouse, Genome Informatics) (supplementary material Fig. S2A). These results indicate that *Irx6* is expressed in a subset of retinal ganglion cells and bipolar cells. *Irx6* also appeared to be transiently expressed in newly born photoreceptor cells (Fig. 2H, inset), but not in adult photoreceptor cells (Fig. 2I).

***Irx6*^{+/*lacZ*} is expressed in a subset of OFF bipolar cells**

To determine the identity of the bipolar cell types that express the *Irx6*^{+/*lacZ*} reporter, retinal sections of *Irx6*^{+/*lacZ*} mice were co-immunolabeled for *Irx6*: β gal and a series of bipolar cell type specific markers (Figs 1, 3). *Irx6*: β gal co-immunolabeled in a subset of cells expressing two type 2 cell markers, *Nk3r* (Fig. 3A-C) and *recoverin* (Fig. 3D-F) (Ghosh et al., 2004; Haverkamp and Wässle, 2000; Milam et al., 1993). *Irx6*: β gal labeling was also detected in a subset of cells immunolabeled for the type 3 and 5, and the rod bipolar cell marker *Cabp5* (Fig. 3G-I) (Ghosh et al., 2004; Haverkamp et al., 2003). Type 3 cells are defined by their

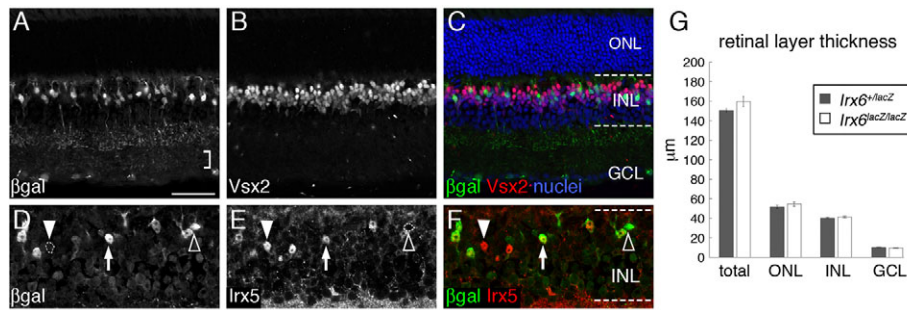


Fig. 4. $Irx6^{lacZ/lacZ}$ mice have normal retinal morphology. (A) Immunolabeling for β gal in the $Irx6^{lacZ/lacZ}$ mouse. Bracket indicates immunolabeling in the ON sublamina of the retina. (B) Immunolabeling for Vsx2. (C) Merged image of A and B, including Draq5 labeling of nuclei in the $Irx6^{lacZ/lacZ}$ mouse. (D-F) $Irx6:\beta$ gal (D) and $Irx5$ (E) expression in the $Irx6^{lacZ/lacZ}$ mouse, showing $Irx6:\beta$ gal expression in a subset of $Irx5$ -positive bipolar cells (F); an $Irx6:\beta$ gal-negative, $Irx5$ -positive (closed arrowhead) bipolar cell; $Irx6:\beta$ gal-positive, $Irx5$ -positive (arrow) bipolar cell; and $Irx6:\beta$ gal-positive, $Irx5$ -negative (open arrowhead) bipolar cell. INL, inner nuclear layer; ONL, outer nuclear layer; GCL, ganglion cell layer. Scale bar: 50 μ m in A-C; 25 μ m in D-F. (G) Retinal thickness in $Irx6^{+/lacZ}$ and $Irx6^{lacZ/lacZ}$ mice ($n=6$ retinas, each genotype). Data are mean \pm s.e.m.

morphology (Ghosh et al., 2004), but can be further categorized into two distinct cell types (type 3a and type 3b) based on their differential immunolabeling for Hcn4 and PKARII β (Prkar2b – Mouse Genome Informatics), respectively (Mataruga et al., 2007). $Irx6:\beta$ gal was detected in type 3a cells co-immunolabeled with Hcn4 (Fig. 3J-L), but not in PKARII β -positive type 3b cells (Fig. 3M-O). Furthermore, $Irx6:\beta$ gal expression was not detected in type 4 cells immunolabeled for calsenilin (Haverkamp et al., 2008) (supplementary material Fig. S2B), or in rod bipolar cells identified by PKC α immunolabeling (Haverkamp and Wässle, 2000; Negishi et al., 1988) (Fig. 3P-R). In summary, within the bipolar cell population of the mature retina, $Irx6$ knock-in reporter gene expression is observed in type 2 and 3a bipolar cells.

Loss of $Irx6$ does not disrupt retinal morphology or number of retinal ganglion cells

To examine the role of $Irx6$ during retinal development, we next examined the phenotype of $Irx6^{lacZ/lacZ}$ mice. Loss of $Irx6$ did not disrupt the gross morphology and layering of the retina (Fig. 4C,G). $Irx6:\beta$ gal immunolabeling was evident in a subset of Vsx2-positive bipolar cells and ganglion cells (Fig. 4A-C) and was visibly more robust than in the $Irx6^{+/lacZ}$ retina (Fig. 2I). In addition to the presence of $Irx6:\beta$ gal in the OFF sublamina of the inner plexiform layer, immunolabeling was also detected in the ON sublamina of the $Irx6^{lacZ/lacZ}$ retina (Fig. 4A; see below). Similar to the $Irx6^{+/lacZ}$ retina, $Irx5$ and $Irx6:\beta$ gal immunolabeling exhibited overlapping and non-overlapping expression patterns in the $Irx6^{lacZ/lacZ}$ retina (Fig. 4D-F).

Since reporter expression indicated that $Irx6$ is expressed in retinal ganglion cells (Fig. 2E,G,H; supplementary material Fig. S2A), we investigated whether ganglion cell number was affected in the $Irx6^{lacZ/lacZ}$ retina. We did not observe a difference in the number of Brn3b positive ganglion cells between the $Irx6^{+/lacZ}$ (10.3 cells/100 μ m \pm 0.6) and $Irx6^{lacZ/lacZ}$ (10.6 cells/100 μ m \pm 0.4) retina ($n=3$ mice).

$Irx6$ is required for the terminal differentiation of OFF bipolar cells

Given that the $Irx6:\beta$ gal reporter is expressed in a subset of OFF bipolar cells, we next examined whether the formation of these cell types was affected in $Irx6^{lacZ/lacZ}$ mice. Loss of $Irx6$ led to the complete loss of recoverin in type 2 cells (Fig. 5A,B). Synaptotagmin II (Syt2) expression, which labels type 2 and 6

bipolar cells (Fox and Sanes, 2007; Wässle et al., 2009), was greatly reduced in the $Irx6^{lacZ/lacZ}$ retina (Fig. 5C,D). Reduced Syt2 immunolabeling of axon termini in the inner plexiform layer was observed for both putative type 2 and 6 bipolar cells (Fig. 5C,D). Axon terminals of Syt2-labeled putative type 6 cells in $Irx6^{lacZ/lacZ}$ mice co-immunolabeled with $Irx6:\beta$ gal (supplementary material Fig. S3), suggesting that the defects in this cell type are cell-autonomous. In contrast to the reduction in recoverin and Syt2 expression, Nk3r immunolabeling of type 1 and 2 cells was still present in the $Irx6^{lacZ/lacZ}$ retina (Fig. 5E,F).

As $Irx6:\beta$ gal is also expressed in type 3a bipolar cells, we next examined whether this cell type was affected by the loss of $Irx6$. In $Irx6^{lacZ/lacZ}$ mice, we observed a specific reduction in the level of Cabp5 immunolabeling within the OFF region corresponding to the position where type 3 axon terminals are located (Fig. 5G,H). Cabp5 immunolabeling of putative type 5 and rod bipolar cell axon terminals was unaffected (Fig. 5G,H). The identification of a Cabp5 immunolabeling defect in type 3 cells was correlated with a slight, but statistically significant, decrease in the number of cells expressing the type 3a cell marker Hcn4 (Fig. 6B,H; Fig. 8I). Furthermore, within the cell bodies of the Hcn4-expressing type 3a cells in the $Irx6^{lacZ/lacZ}$ retina, a loss of Cabp5 immunolabeling was observed (Fig. 6C,D,I,J). The reduction of Cabp5 immunolabeling was specific to type 3a cells and was not observed in PKARII β -positive type 3b cells (Fig. 6E,F,K,L; data not shown). Together, these results identify a specific defect in type 3a bipolar cells of the $Irx6^{lacZ/lacZ}$ retina marked by a loss of Cabp5 immunolabeling and a reduction in the total number of Hcn4-expressing bipolar cells.

Hcn4-expressing OFF bipolar cells exhibit stratification defects in $Irx6$ mutant mice

In addition to a reduction in the number of Hcn4-immunolabeled putative type 3a bipolar cells in the $Irx6^{lacZ/lacZ}$ retina, we observed defects in the stratification of the remaining Hcn4-immunolabeled axon terminals (Fig. 6H; Fig. 7). These defects were characterized by the expansion of Hcn4-immunolabeled axon terminals into the entire OFF region of the inner plexiform layer (Fig. 7B,C). To determine more precisely the nature of this defect, we performed co-immunolabeling experiments with calretinin, a marker used to distinguish specific inner plexiform layer sublaminae (Ghosh et al., 2004; Haverkamp and Wässle, 2000). The five distinct sublaminae defined by calretinin immunolabeling were unaltered in the $Irx6^{lacZ/lacZ}$ retina (Fig. 7H,I). The axon terminals of type 3 bipolar

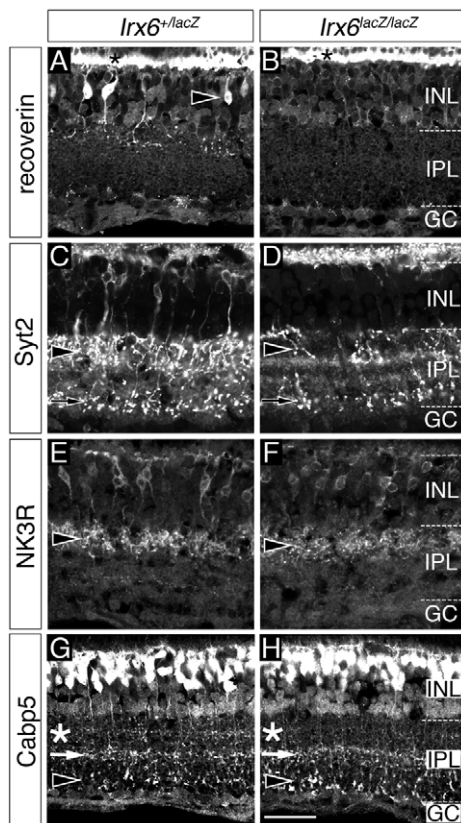


Fig. 5. OFF cone bipolar cell gene expression defects in *Irx6:βgal* mice. (A–D) Recoverin (A,B) and synaptotagmin 2 (C,D) immunolabeling of type 2 cells (arrowheads in A,C,D) is reduced in *Irx6^{lacZ/lacZ}* mice. The asterisks in A,B indicate recoverin immunolabeling of photoreceptor cells. Synaptotagmin 2 immunolabeling of the axon terminals of type 6 cells is also reduced in *Irx6^{lacZ/lacZ}* mice (arrows in C,D). (E,F) Nk3r immunolabeling is not reduced in *Irx6^{lacZ/lacZ}* mice, as judged by labeling of soma and axon terminals (arrowheads). (G,H) Cabp5 expression is reduced in the region of the inner plexiform layer normally occupied by the axon terminals of type 3 cells (compare asterisks in G and H), but is unaffected in the axon terminal of type 5 (arrows in G and H) and rod bipolar cells (arrowheads in G and H) in the *Irx6^{lacZ/lacZ}* mouse. INL, inner nuclear layer; IPL, inner plexiform layer; GC, ganglion cell layer. Scale bar: 25 μm.

cells are normally positioned in sublamina 2 (between the two outermost calretinin-labeled bands), whereas the axon terminals of type 1 and 2 bipolar cells are positioned within sublamina 1, located above the outermost calretinin-labeled band (Ghosh et al., 2004). In contrast to the invariable positioning of Hcn4-immunolabeled axon terminals in sublamina 2 in the wild-type (data not shown) and *Irx6^{+/lacZ}* retina (Fig. 7D–F), we observed Hcn4 immunolabeling spanning both sublamina 1 and 2 in *Irx6^{lacZ/lacZ}* mice (Fig. 7G–I). This expansion of Hcn4-labeled termini in *Irx6^{lacZ/lacZ}* mice was observed across the entire retina. Hcn4-labeled axon terminals were not observed in sublaminae 3–5, where ON bipolar cell axon terminals reside (Fig. 7G–I). In support of the observation of expanded Hcn4-immunolabeled axon termini, we measured a slight but statistically significant increase in the ratio of fluorescence intensity between a region of interest located directly below the inner nuclear layer (sublamina 1) and region of equal size located immediately below and corresponding to sublamina 2 (0.84 ± 0.02 for *Irx6^{+/lacZ}* retina; 0.90 ± 0.02 for

Irx6^{lacZ/lacZ} retina; $n=5$, $P<0.03$), suggesting that there is a shift in the axon stratification of putative type 3a bipolar cells in the *Irx6^{lacZ/lacZ}* mouse. These results suggest that *Irx6* is required for the correct axon stratification of Hcn4-expressing cells within the OFF sublamina of the inner plexiform layer.

Dysregulation of *Vsx1* and *Bhlhb5* in *Irx6* mutant mice

The OFF bipolar cell axon stratification defects observed in putative type 3a bipolar cells of *Irx6^{lacZ/lacZ}* mice raises the possibility that OFF bipolar cell subtype identity is affected in the *Irx6* mutant. We therefore asked whether the expression of *Vsx1* and *Bhlhb5*, two transcription factors required for OFF bipolar cell differentiation, was affected in *Irx6^{lacZ/lacZ}* mice. *Vsx1* expression is undetectable in Hcn4-positive type 3a cells in the wild-type retina (Shi et al., 2012). In the *Irx6^{+/lacZ}* retina, *Vsx1* was normally not detected in Hcn4-expressing type 3a cells (Fig. 8C), but in rare instances, Hcn4-positive bipolar cells exhibited faint levels of *Vsx1* immunolabeling (data not shown). By contrast, in the *Irx6^{lacZ/lacZ}* retina, ectopic *Vsx1* immunolabeling was prominent in Hcn4-expressing bipolar cells (Fig. 8B,D,H). Despite the presence of ectopic *Vsx1* immunolabeling, there was no significant change in the number of *Vsx1*-labeled cells in *Irx6^{lacZ/lacZ}* mice (Fig. 8I). Unlike *Vsx1*, a significant reduction in the level of *Bhlhb5* immunolabeling of type 2 cells was observed in the bipolar cell region of the inner nuclear layer in *Irx6^{lacZ/lacZ}* mice (Fig. 8E,F,I). A previously uncharacterized subset of Hcn4-positive type 3a cells in wild-type and *Irx6^{+/lacZ}* mice that weakly co-immunolabeled for *Bhlhb5* was also reduced in size in the *Irx6^{lacZ/lacZ}* retina (Fig. 8E; data not shown). The population of *Bhlhb5*-positive amacrine cells, identified by both position and co-immunolabeling with the amacrine cell marker syntaxin, remained unchanged in the absence of *Irx6* (Fig. 8E,F). These data demonstrate a differential requirement for *Irx6* in the regulation of *Bhlhb5* and *Vsx1* such that *Irx6* is required for the repression of *Vsx1* in type 3a cells and for the activation of *Bhlhb5* in type 2 and 3a bipolar cells.

Mixed subtype identity in Hcn4-expressing OFF bipolar cells in the *Irx6*-mutant retina

As *Vsx1* is necessary for the expression of several type 2 bipolar cell-specific markers (Chow et al., 2004; Ohtoshi et al., 2004), we next examined the possibility that the presence of ectopic *Vsx1* in Hcn4-expressing cells in the *Irx6*-mutant was correlated with the ectopic expression of type 2 markers regulated by *Vsx1*. We focused our attention on the type 1 and 2 bipolar cell marker Nk3r, because, unlike recoverin, its expression is not lost in the *Irx6* mutant (Fig. 5E,F). In the wild type, *Irx6^{+/lacZ}* and *Irx6^{+/lacZ};Vsx1^{+/Altb5}* double heterozygous retina, Nk3r and Hcn4 are expressed in a mutually exclusive manner in presumptive type 1, 2 and 3a cells, respectively (Fig. 9A–C',J; data not shown). In both the *Irx6^{lacZ/lacZ}* and *Irx6^{lacZ/lacZ};Vsx1^{+/Altb5}* retina, ectopic Nk3r immunolabeling was observed in Hcn4-immunolabeled cell somas (Fig. 9D–F,J; data not shown) and in the axon terminals of putative type 3a cells (Fig. 9D'–I'). A population of Nk3r-positive putative type 1 or 2 cells was not labeled with Hcn4 (Fig. 9D–F). In agreement with our observation of co-immunolabeling between Hcn4 and Nk3r in the *Irx6^{lacZ/lacZ}* retina, we measured a significant increase in the number of Nk3r-positive bipolar cells in the *Irx6^{lacZ/lacZ}* retina when compared with the *Irx6^{+/lacZ}* retina (Fig. 8I). We also observed a decrease in the fluorescence intensity ratio between sublamina 1 and 2 for Nk3r immunolabeling in the *Irx6^{lacZ/lacZ}* retina (1.2 ± 0.07) when compared with the *Irx6^{+/lacZ}*

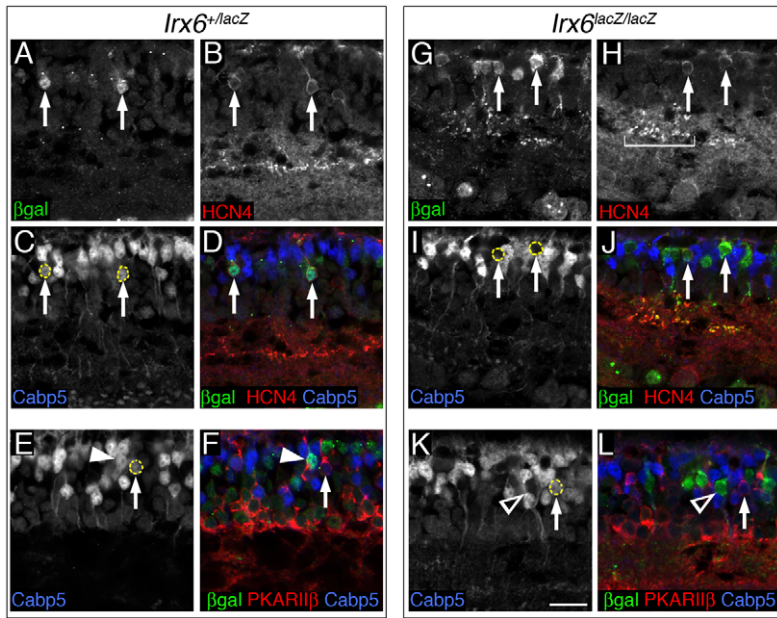


Fig. 6. *Irx6^{lacZ/lacZ}* mice have a reduction in *Cabp5* staining in type 3a bipolar cells. (A-L) *Irx6^{+/lacZ}* (A-F) and *Irx6^{lacZ/lacZ}* mice (G-L) were immunolabeled for *Irx6:βgal* (A,G), *Hcn4* (B,H) and *Cabp5* (C,I). Arrows indicate cells in the heterozygous retina (A-D) that are positive for *Irx6:βgal*, *Hcn4* and *Cabp5*, and cells in the *Irx6^{lacZ/lacZ}* retina (G-J) that are *Irx6:βgal* and *Hcn4* positive, but have lost *Cabp5* expression. Bracket in H indicates *Hcn4* staining in the inner plexiform layer of the mutant mouse. Staining for *Irx6:βgal* (E,K) and *PKARIIβ* (F,L) shows that there is no change in the colocalization of these markers with *Cabp5* in the heterozygous and *Irx6^{lacZ/lacZ}* mouse. Arrows in E,F,K,L indicate cells that are positive for *Cabp5* and *PKARIIβ* expression. Arrowheads in E,F,K,L indicate *Irx6:βgal*-expressing cells that are positive (E,F) or negative (K,L) for *Cabp5*. Scale bar: 12 μ m.

retina (1.5 ± 0.1 ; $P < 0.03$, $n = 3$ mice), providing further support for the finding that there is an increase in *Nk3r* immunolabeling in sublamina 2. Together, these findings suggest that *NKR3* is ectopically expressed in putative type 3a bipolar cells in both the *Irx6^{lacZ/lacZ}* and *Irx6^{lacZ/lacZ}; Vsx1^{+/AltB5}* retina.

Given that both *Nk3r* and *Hcn4* are downregulated in the *Vsx1*-null retina (Chow et al., 2004; Shi et al., 2012), we next asked whether their co-expression in putative type 3a bipolar cells of the *Irx6* mutant retina would be affected in mice deficient for both *Irx6* and *Vsx1*. Unexpectedly, despite the predicted reduction in overall immunolabeling of the two markers *Hcn4* and *Nk3r*, co-immunolabeled bipolar cells were still observed in the *Irx6^{lacZ/lacZ}; Vsx1^{AltB5/AltB5}* double homozygous mutant retina (Fig. 9G-J). In the *Irx6^{lacZ/lacZ}; Vsx1^{AltB5/AltB5}* mutant retina, all of the *Hcn4*-expressing bipolar cells co-immunolabeled with *Nk3r* (Fig. 9J). These data indicate that the expression of *Nk3r* in *Hcn4*-expressing cells appears to be independent of *Vsx1*. We also observed a population of *Nk3r*-positive cells that did not label with *Hcn4* in the *Irx6^{lacZ/lacZ}; Vsx1^{AltB5/AltB5}* double homozygous mutant retina. In agreement with previous findings in the *Vsx1*-null retina (Chow et al., 2004), we observed a decrease in the number of *Nk3r* immunolabeled cells in the *Irx6^{+/lacZ}; Vsx1^{AltB5/AltB5}* retina when compared with the *Irx6^{+/lacZ}; Vsx1^{+/AltB5}* retina (Fig. 9J). In the *Irx6^{lacZ/lacZ}; Vsx1^{AltB5/AltB5}* double homozygous mutant retina we observed a further decrease in the number of *Nk3r*-only immunolabeled cells (Fig. 9J), suggesting that *Irx6* and *Vsx1* can both induce *Nk3r* expression.

To determine whether *Vsx1* expression has an effect on the expression of the *Irx6*, we examined the expression of the *Irx6:βgal* reporter in the presence and absence of *Vsx1*. There was a significant increase in the number of *Irx6:βgal* positive cells in the *Irx6^{+/lacZ}; Vsx1^{AltB5/AltB5}* retina when compared with the *Irx6^{+/lacZ}; Vsx1^{+/AltB5}* retina (Fig. 9K). These results suggest that *Vsx1* has a partial inhibitory effect on the expression of *Irx6*.

Irx6* can activate or repress transcription through Iroquois-binding sites found proximal to recoverin, *Vsx1* and *Nk3r

Members of the Iroquois family are known *in vitro* to a DNA sequence known as the Iroquois-binding site (IBS) and

function as transcriptional repressors (Bilioni et al., 2005; Berger et al., 2008). To gain insight into the molecular mechanism by which the expression of the OFF bipolar cell markers recoverin, *Vsx1* and *Nk3r* is disrupted in the *Irx6^{lacZ/lacZ}* mouse, we searched for candidate sequences that match the IBSs in the regions

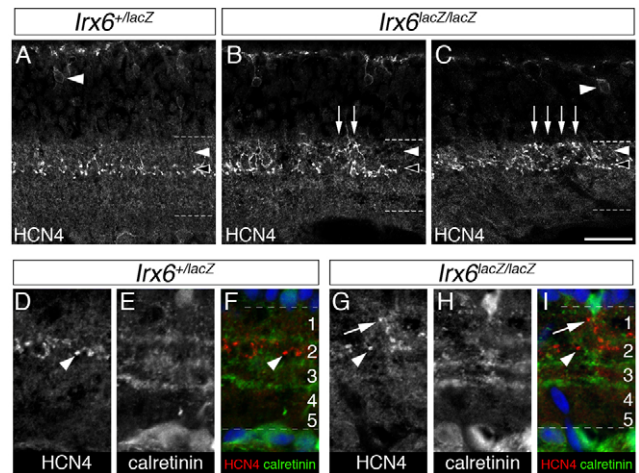


Fig. 7. Abnormal distribution of *Hcn4* immunolabeling in the inner plexiform layer of the *Irx6^{lacZ/lacZ}* retina.

(A-C) Immunolabeling for *Hcn4* in the *Irx6^{+/lacZ}* (A) and *Irx6^{lacZ/lacZ}* (B,C) retina. Arrowheads indicate *Hcn4*-positive cell bodies in the inner nuclear layer of the retina. Arrows indicate increased expression of *Hcn4* in the upper zone of the inner plexiform layer. Broken lines define the boundary of the inner plexiform region (A-C,F,I).

(D-I) Immunolabeling using calretinin to further define the projection zones of the inner plexiform region of the retina. In the *Irx6^{+/lacZ}* retina, *Hcn4* immunolabeled axon terminals of putative type 3a cells (D) are restricted to sublamina 2 in the inner plexiform layer, as defined by calretinin immunolabeling (E). Arrowheads (D,F) indicate *Hcn4*-positive axon termini in sublamina 2. By contrast, in the *Irx6^{lacZ/lacZ}* retina (G-I), *Hcn4* immunolabeling (G) is detected in both sublamina 1 and 2, as defined by calretinin immunolabeling (H). *Hcn4*-positive axon termini in sublamina 1 (G,I, arrows) and sublamina 2 (G,I, arrowheads). Scale bar: 25 μ m in A-C; 18 μ m in D-I.

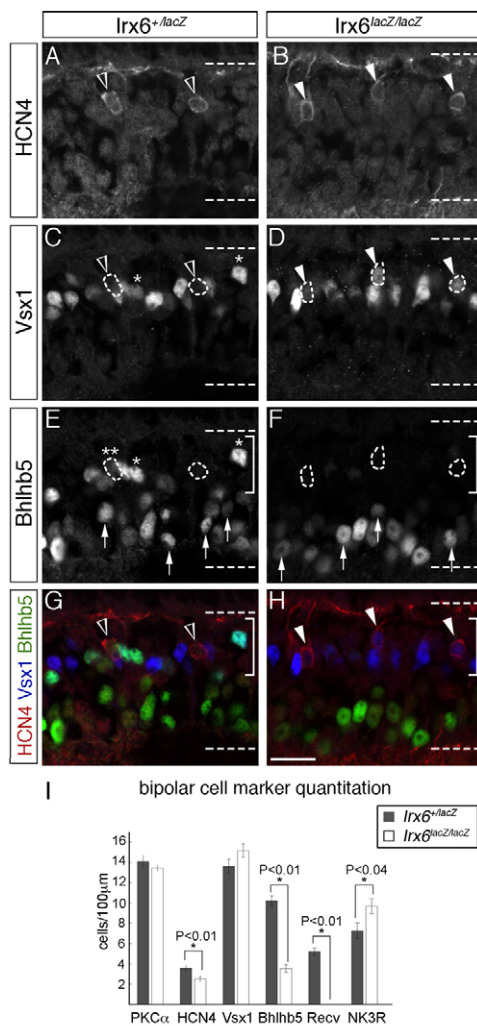


Fig. 8. *Irx6* regulates the expression of transcription factors required for OFF bipolar cell development. (A-H) *Vsx1* immunolabeling is ectopically upregulated in Hcn4-expressing cells (A,B, arrowheads) in the *Irx6*^{lacZ/lacZ} retina (compare C,D, arrowheads). The single asterisks in C and E indicate a putative type 2 cell, based on its co-labeling of *Vsx1* and *Bhlhb5* and on the lack of *Hcn4* immunolabeling. In the *Irx6*^{lacZ/lacZ} retina, *Bhlhb5* immunolabeling of the bipolar cell region of the inner nuclear layer (indicated by the bracketed regions in E-H) is greatly reduced compared with the *Irx6*^{+/lacZ} retina (E,F). Amacrine cell labeling of *Bhlhb5* (E,F, arrows) is retained in the *Irx6*^{lacZ/lacZ} retina. An example of a putative type 3a cell expressing low levels of *Bhlhb5* is indicated by the double asterisk in E. Scale bar in H: 15 µm. (I) Quantitation of bipolar cell marker expression in the retina of *Irx6*^{+/lacZ} ($n=5$ retinas) and *Irx6*^{lacZ/lacZ} ($n=6$ retinas) mice. Recv, recoverin. Data are mean±s.e.m.

proximal to these genes. Candidate IBSs in *Vsx1*, *Tacr3* (the gene encoding Nk3r) and *Rcvrn* were identified (Fig. 10A; supplementary material Table S2). We then performed a series of transcriptional reporter assays to determine whether *Irx6* might directly regulate the expression of these factors. Regions of ~200 bp of *Vsx1* or *Tacr3* surrounding the predicted IBSs were cloned upstream of an SV40 promoter-driven luciferase reporter plasmid. In three of the four IBS sequences examined, we observed repression of luciferase expression in the presence of co-transfected *Irx6* (Fig. 10B). Upstream of *Rcvrn* we identified a fragment containing a potential IBS (Fig. 10A), and positioned a 1.3 kb

region containing this site in front of a mini-promoter-driven luciferase reporter construct (supplementary material Table S2). Unexpectedly, in contrast to the well-characterized repressor activity of *Irx* transcription factors, reporter assays showed that the addition of *Irx6* had an activating effect on transcription of the *Rcvrn* reporter (Fig. 10C). Interestingly, addition of *Irx5* had no effect on transcription and did not alter *Irx6*-mediated activation (Fig. 10C). Together, these findings suggest that *Irx6* can function in a context-dependent manner as either a transcriptional repressor or activator, and may explain the increased expression of *Vsx1*/*Nk3r* and decreased expression of recoverin in the *Irx6*^{lacZ/lacZ} mouse.

Visual signaling defects in *Irx6* mutant mice

To determine whether the retinal defects in *Irx6* mutant mice were accompanied by defects in visual signaling, electroretinography (ERG) was performed on mice at 3–4 months of age. In contrast to wild-type and *Irx6*^{+/lacZ} mice, *Irx6*^{lacZ/lacZ} mice exhibited a reduction of dark-adapted and light-adapted a-wave amplitude (Fig. 11A; data not shown), which reflects photoreceptor activity. Consistent with the reduced a-wave amplitude, a decreased ERG b-wave amplitude, which is indicative of post photoreceptor retinal activity, was also observed (Fig. 11C). No changes were observed in a-wave or b-wave kinetics (Fig. 11B,D), suggesting that the biochemical integrity of the photoreceptors and inner retina was not lost. Despite the presence of OFF bipolar differentiation defects in *Irx6*^{lacZ/lacZ} mice, light-adapted OFF responses were intact in *Irx6*^{lacZ/lacZ} mice compared with controls (Fig. 11E,F; data not shown). In summary, *Irx6*^{lacZ/lacZ} mice exhibit a reduced ERG a-wave and b-wave, but have intact light-adapted OFF visual signaling responses.

DISCUSSION

Here, we show that *Irx6* is required downstream of bipolar cell specification for the terminal differentiation of type 2, type 3a and possibly type 6 bipolar cells (Fig. 12A).

Our results suggest there is a complex regulatory network of transcription factors (i.e. *Irx6*, *Vsx1* and *Bhlhb5*) that function to regulate the development of type 2 and 3a bipolar cells (Fig. 12B). In the *Irx6*^{lacZ/lacZ} mutant mouse, type 2 cells have reduced recoverin and *Bhlhb5* immunolabeling, but retain *Vsx1* and some *Nk3r* immunolabeling. In the *Irx6*;*Vsx1* homozygous mutant mouse, we see a decrease in the number of *Nk3r* alone-positive cells compared with either the *Irx6*^{+/lacZ};*Vsx1*^{AltB5/AltB5} mouse or *Irx6*^{lacZ/lacZ};*Vsx1*^{+/AltB5} mouse. This genetic interaction reveals that both *Irx6* and *Vsx1* contribute to the expression of *Nk3r* in type 2 cells in the mouse retina. Based on our observations and published work (Chow et al., 2004; Feng et al., 2006; Kerschensteiner et al., 2008; Ohtoshi et al., 2004), we suggest that both *Vsx1* and *Bhlhb5* have a central role in directing the terminal differentiation and maturation of type 2 bipolar cells, with *Irx6* taking on a more minor role in regulating the formation of this cell type (Fig. 12B).

In type 3a bipolar cells, our findings reveal that *Irx6* has a key role in defining cell type specific gene expression. Results from the transcriptional reporter assays suggest that *Irx6* could directly repress the expression of both *Vsx1* and *Nk3r*, and therefore is likely to be responsible in part for repressing the expression of these genes in type 3a cells. Members of the *Irx* family have been shown to act as transcriptional repressors (Bilioni et al., 2005; Costantini et al., 2005). Although the measured increase in *Vsx1* immunolabeling in the *Irx6*^{lacZ/lacZ} retina was not statistically significant, we think this is due to *Vsx1* also being expressed in

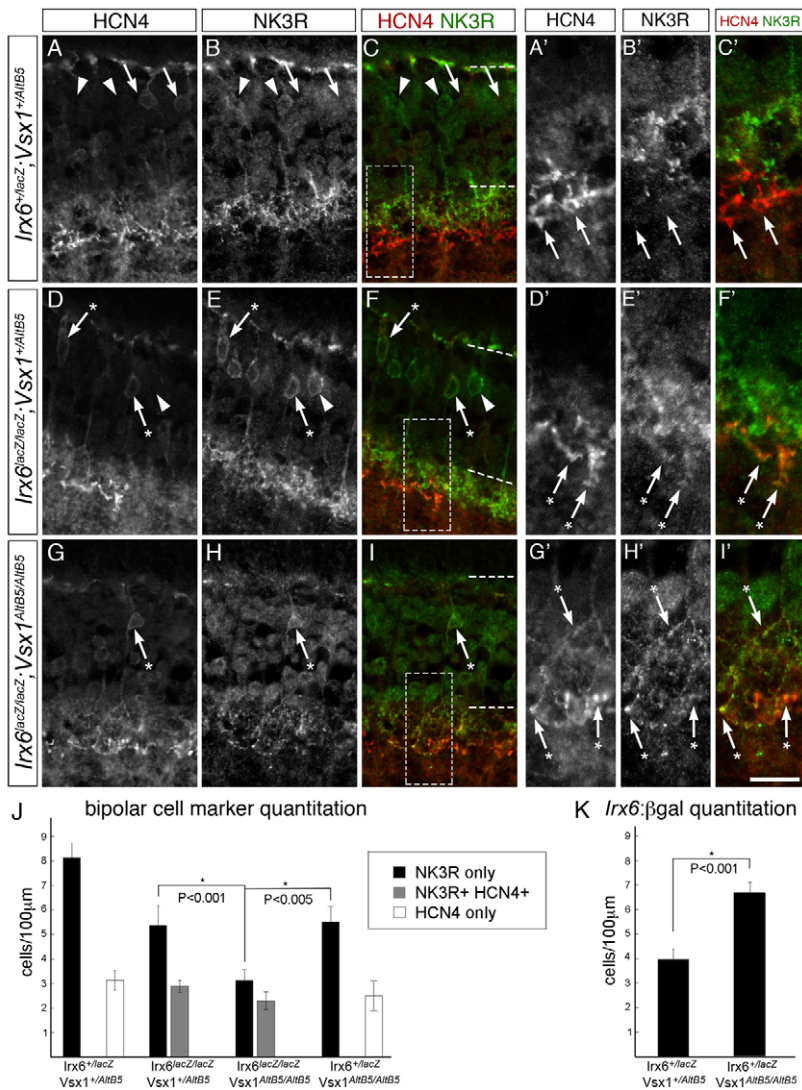


Fig. 9. Co-labeling of Nk3r in putative type 3a bipolar cells in the *Irx6^{lacZ/lacZ}* retina. (A-C) In the *Irx6^{+/lacZ};Vsx1^{+/Altb5}* retina (A-C), Nk3r and Hcn4 immunolabeling of putative types 1 or 2 (arrowheads) and type 3a (arrows) cells, respectively, does not overlap in cell somas or axon terminals (A'-C'). (D-F') By contrast, in the *Irx6^{lacZ/lacZ};Vsx1^{+/Altb5}* retina, Hcn4 immunolabeling in putative type 3a cells that exhibit type 3a axon stratification are co-immunolabeled with Nk3r (indicated by cells with asterisked arrows). Putative type 1 or 2 cells expressing only Nk3r and not Hcn4 are labeled with an arrowhead. (G-I') In the *Irx6^{lacZ/lacZ};Vsx1^{Altb5/Altb5}* retina, co-labeling of Hcn4 and Nk3r is observed in the cell soma (indicated by asterisked arrows) and in the inner plexiform layer. Scale bar: 15 μm in A-I; 10 μm in A'-I'. (J) Quantitation of bipolar cells immunolabeled with Nk3r alone (black), Nk3r and Hcn4 (gray), and Hcn4 alone (white) in the retina of *Irx6^{+/lacZ};Vsx1^{+/Altb5}*, *Irx6^{lacZ/lacZ};Vsx1^{+/Altb5}*, *Irx6^{lacZ/lacZ};Vsx1^{Altb5/Altb5}* and *Irx6^{+/lacZ};Vsx1^{Altb5/Altb5}* mice (n=3, 3, 4, 2 mice, respectively). (K) Quantitation of *Irx6*:βgal expression in the retina of *Irx6^{+/lacZ};Vsx1^{+/Altb5}* and *Irx6^{+/lacZ};Vsx1^{Altb5/Altb5}* mice (n=3 mice for both genotypes). Data are mean±s.e.m.

type 7 bipolar cells, and that any increase in *Vsx1*-positive cell number in the *Irx6^{lacZ/lacZ}* retina is masked by the additional expression of *Vsx1* in the ON bipolar cells.

Irx6 also promotes the expression of *Bhlhb5* and *Cabp5*, and partially promotes the expression of *Hcn4* in type 3a cells. In the *Irx6^{lacZ/lacZ}* mouse retina, we observe a 'hybrid' cell that shows characteristics of both type 2 and 3a bipolar cells, and extends axon terminal projections throughout the OFF sublamina, suggesting that *Irx6* expression is necessary to generate a type 3a bipolar cell with a separate identity from a type 2 cell (Fig. 12B). We propose that, in the *Irx6^{lacZ/lacZ}* mouse, the type 3a bipolar cells adopt molecular features of type 2 cells, as we observe a large increase in the total number of Nk3r immunolabeled cells in the *Irx6^{lacZ/lacZ}* retina. This increase in Nk3r immunolabeled cells is consistent with the ectopic expression of Nk3r in Hcn4-positive type 3a cells, but would not be expected if Nk3r immunolabeled type 1 or 2 cells ectopically expressed Hcn4. Additionally, in both the *Irx6^{lacZ/lacZ}* and *Irx6;Vsx1* double homozygous mutant retinas, we observe *Irx6*:βgal cells that are either positive for Hcn4 (and Nk3r) or negative for Hcn4, suggesting that there are two types of *Irx6*:βgal reporter cells in the *Irx6^{lacZ/lacZ}* mouse (supplementary material Fig. S4). The putative type 2/3a hybrid cell is still present in the retina of the *Irx6;Vsx1* homozygous mutant mouse, even in the absence of robust *Bhlhb5*

bipolar cell expression (supplementary material Fig. S4), suggesting that *Irx6* is a primary regulator in controlling the formation of type 3a cells in a mechanism that is independent of *Vsx1* function (Fig. 12B), but that other factors must also be functioning to regulate OFF bipolar cell specific gene expression. Together, these observations support a model in which the identities of type 2 and 3a bipolar cells are defined, in part by opposing, yet interdependent, transcription factor gene expression established in these cell types.

In *Irx6* mutant retinas, recoverin immunolabeling in type 2 bipolar cells was lost. Results from the transcriptional reporter assay suggest that the putative IBS upstream of *Rcvrn* can induce *Irx6*-dependent transcriptional activation, and this is consistent with our genetic data showing loss of recoverin in the *Irx6^{lacZ/lacZ}* mouse. In *Irx5* mutant retinas, recoverin immunolabeling in type 2 cells is also downregulated, demonstrating that *Irx5* and *Irx6* are not functionally redundant. As we did not observe any effect in our transcriptional assay with the addition of *Irx5*, the *Rcvrn* transcriptional activation site for *Irx5* remains unclear, and our data suggest that the function of putative Iroquois-binding sites is highly dependent on the surrounding sequence.

Although no ganglion cell defects were observed in *Irx6^{lacZ/lacZ}* mice (supplementary material Fig. S5), nor in the individual *Irx2*,

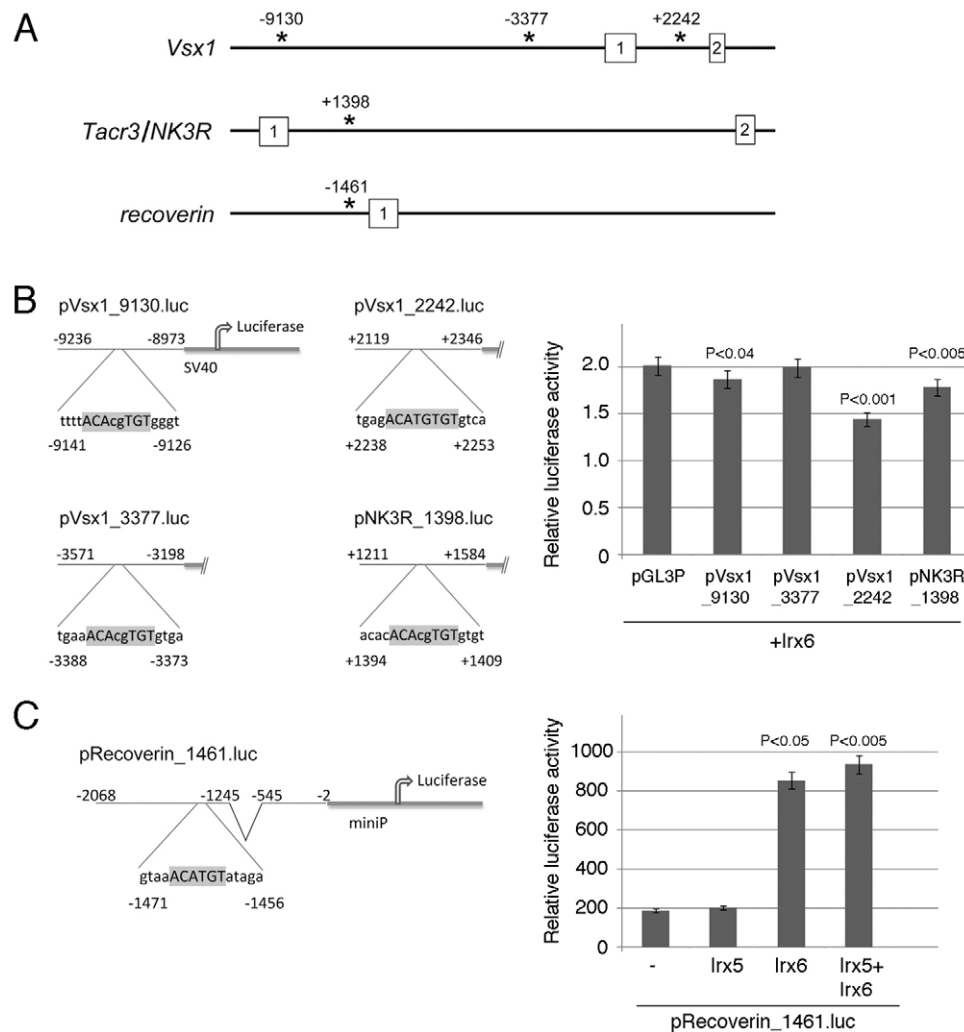


Fig. 10. *Irx6* can act as a transcriptional repressor or activator on sites found proximal to OFF bipolar cell markers. (A) Potential IBS found proximal to *Vsx1*, *Tacr3* (*Nk3r*) and *Rcvrn*. Numbered boxes indicate exons. (B,C) *Irx6* represses both *Vsx1*-luciferase (B) and *Nk3r*-luciferase and activates *Rcvrn*-luciferase (C) expression in HEK cells. Data are mean \pm s.e.m.

Irx4 or *Irx5* gene knockout mice (Bruneau et al., 2001; Cheng et al., 2005; Lebel et al., 2003) previous studies in chick suggest a role for Iroquois genes in these cells (Jin et al., 2003). Although in situ hybridization studies have shown that ganglion cells express both *IrxA* and *IrxB* cluster genes, only the Iroquois cluster B genes are expressed in the bipolar cell region of the inner nuclear layer (Cohen et al., 2000) (R.L.C., unpublished). This difference in expression could explain why defects are observed in bipolar cells and not in ganglion cells of both *Irx6* and *Irx5* mutants, and suggests that the absence of a ganglion cell phenotype in individual *Irx* loss-of-function mutants is due to functional redundancy of the *Irx* proteins.

Iroquois genes appear to have a conserved function in subdividing neuronal projection domains. In the *Drosophila* notum, the *Iro* complex appears to control axonal projections of medial versus lateral mechanosensory bristles (Grillenzoni et al., 1998). In addition, the *Iro* complex prevents dorsal photoreceptor axons from misprojecting to the ventral lamina by inhibiting *Drosophila* *Wnt4* (Sato et al., 2006). Similar to the fly, our results reveal that *Irx6* functions in subdividing neuronal projection domains in the mammalian retinal inner plexiform layer. In *Irx6*^{lacZ/lacZ} mice, axonal projections of presumptive type 3a bipolar cells, which are

normally restricted to sublamina 2, are also observed in sublamina 1. Interestingly, the presumptive type 3a cells did not misproject to sublamina 3-5, where the axon terminals of ON bipolar cells reside. This observed axonal termini misprojection phenotype is reminiscent of the *Sema5a*^{-/-}; *Sema5b*^{-/-} mouse retinal phenotype, where *Cabp5* immunolabeled type 3 bipolar cells also had ectopic projections to sublamina 1 (Matsuoka et al., 2011). These findings suggest that at least two mechanisms are required for bipolar cell type axonal development: one that defines the division of ON versus OFF boundaries; and one (involving *Irx6*) that is required for proper positioning within the OFF region. Parallels between the axon guidance defects in the mouse retina and in *Drosophila* suggest a conserved role for *Irx* genes in regulating axon projection domain specificity.

How the loss of *Irx6* affects visual signaling is unclear at this point. In *Irx6* mutants, the ERG b-wave amplitude, an indicator of bipolar cell activity was intact, but reduced. However, as the amplitude of the a-wave (a measure of photoreceptor activity) was also reduced, it was not possible to determine whether the reduced b-wave was due to defects in bipolar cell function. The reduced a-wave amplitude in *Irx6*^{lacZ/lacZ} mice was unexpected. Although a

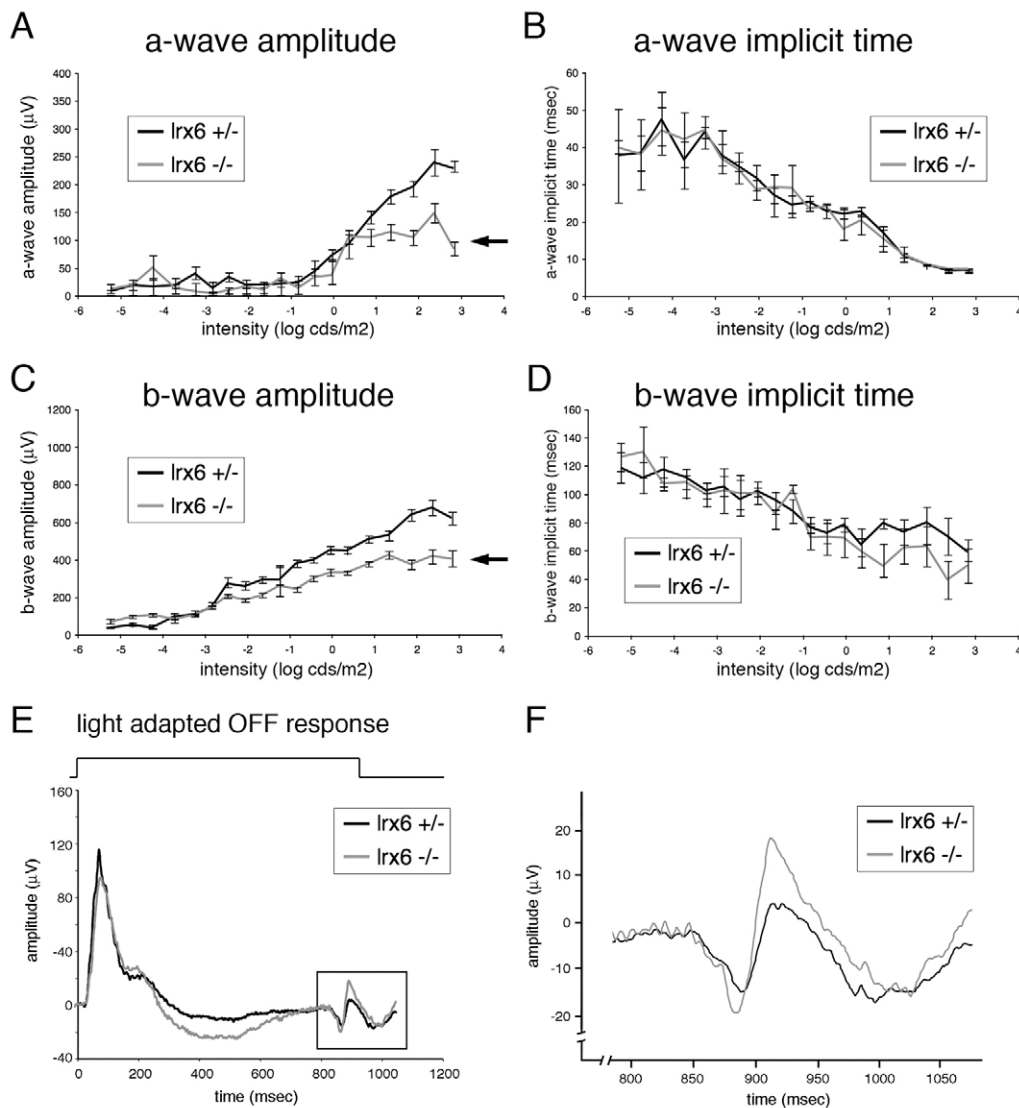


Fig. 11. Visual signaling defects in *Irx6*^{lacZ/lacZ} mice. (A–D) Dark-adapted ERG a-wave (A) and b-wave (C) amplitudes were reduced in *Irx6*^{lacZ/lacZ} ($n=5$) compared with *Irx6*^{+/-} mice ($n=4$). Both the a-wave (B) and b-wave (D) implicit time values were unaffected in *Irx6*^{lacZ/lacZ} mice. Data are mean \pm s.e.m. (E) An example of the light-adapted OFF response in *Irx6*^{lacZ/lacZ} and *Irx6*^{+/-}. (F) The inset in E revealing an intact d-wave that is generated in response to light OFF-set.

reduced a-wave amplitude was previously observed in *Irx5* mutant mice, this was attributed to the overall reduced size of *Irx5* mice compared with controls (Cheng et al., 2005). *Irx6*^{lacZ/lacZ} mice, however, do not exhibit any significant reduction in overall size (data not shown) or photoreceptor layer thickness, raising the possibility that the reduced a-wave amplitude is due to a defect in photoreceptor function. How this defect could be manifest is presently unclear given that the a-wave implicit time kinetics were unaffected in the *Irx6* mutants. Interestingly, transient expression of the *Irx6*: β gal reporter was observed in photoreceptor cells, suggesting that there may be a requirement for *Irx6* during photoreceptor development. The light adapted d-wave, a specific indicator of OFF bipolar cell function, was intact in *Irx6* mutants; this result contrasts the OFF visual signaling defects previously observed in *Vsx1* mutant mice (Chow et al., 2004; Kerschensteiner et al., 2008) and with our observation that *Vsx1*-null mice have a reduced d-wave (data not shown). This difference in visual signaling phenotype is surprising given that the *Vsx1* and *Irx6*

mutants have overlapping gene expression defects in OFF bipolar cells. However, the *Vsx1* and *Irx6* mutant phenotypes are not identical. In particular, *Vsx1* and *Nk3r* expression are upregulated in type 3a bipolar cells in the *Irx6* mutant. Future work examining the signaling properties of *Irx6* and *Vsx1* mutant OFF bipolar cells in isolation and slice preparations will be important to begin to understand how these genes regulate functional differences in OFF bipolar subtypes.

One question that remains unanswered is to what extent the specification of diverse retinal bipolar cell subtypes is driven by intrinsic (i.e. transcription factor coding) and extrinsic mechanisms. Although dissociation studies have suggested that intrinsic factors play a dominant role in regulating E16–17 retinal progenitor cell cycle exit and cell fate determination, these studies have focused on retinal cell classes and not on subtype determination (Cayouette et al., 2003). In the developing neural tube, specification of ventral interneurons is determined in part by a dorsal–ventral Hedgehog signaling gradient that regulates the expression of homeodomain

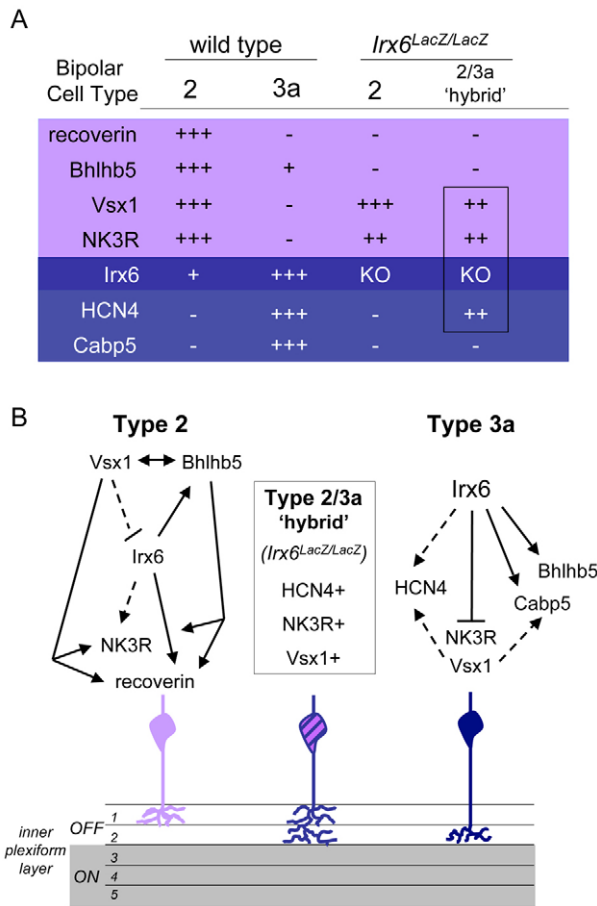


Fig. 12. Regulatory network model of *Irx6*, *Vsx1* and *Bhlhb5* in directing terminal gene expression in OFF bipolar cells.

(A) Expression of type 2 and 3a cell markers in the *Irx6*^{LacZ/LacZ} (wild-type retina), and the resulting changes in marker expression in the *Irx6*^{LacZ/LacZ} retina. (B) We propose that *Vsx1* and *Bhlhb5* are key players in regulating the terminal differentiation and maturation of type 2 cells, while *Irx6* has a leading role in regulating the formation of type 3a cells. *Irx6* is necessary for preventing type 3a cells from adopting type 2 cell characteristics in a mechanism that is independent of *Vsx1* activity. Dashed lines indicate partial repression or activation.

and basic helix-loop-helix transcription factors (Briscoe et al., 2000). As is the case in the retina, subtypes exist within different ventral interneuronal classes of the neural tube that possess distinct axonal targeting properties and neuronal activity (Shirasaki and Pfaff, 2002). Retinal type 7 bipolar cell dendrite stratification is not affected by the absence of photoreceptors (Keeley and Reese, 2010), supporting the idea that intrinsic mechanisms specify some aspects of bipolar cell type development that is independent of extrinsic cues. Future experiments aimed at understanding how *Irx6* and its downstream targets are regulated by intrinsic and extrinsic cues will provide insight into the control of retinal bipolar cell type diversity.

Acknowledgements

We thank F. Haeseleer, R. R. McInnes, F. Müller, A. Hirano and C. C. Hui for reagents and members of the R.L.C. lab for comments and suggestions.

Funding

This work was supported by operating grants from the Canadian Institutes for Health Research, The Foundation Fighting Blindness – Canada (R.L.C.) and National Institutes of Health/National Heart, Lung, and Blood Institute

(NIH/NHLBI) [R01 HL93414 ARRA to B.G.B.]. Y.S. is an Alberta Innovates-Health Solutions (AIHS) Senior Scholar [200800242]. E.N.S. is supported by a Michael Smith Foundation for Health Research Postdoctoral Fellowship. R.L.C. is supported by a Tier 2 Canada Research Chair. Deposited in PMC for release after 12 months.

Competing interests statement

The authors declare no competing financial interests.

Supplementary material

Supplementary material available online at

<http://dev.biologists.org/lookup/suppl/doi:10.1242/dev.081729/-/DC1>

References

- Alvarez, B. V., Gilmour, G. S., Mema, S. C., Martin, B. T., Shull, G. E., Casey, J. R. and Sauvé, Y. (2007). Blindness caused by deficiency in AE3 chloride/bicarbonate exchanger. *PLoS ONE* **2**, e839.
- Berger, M. F., Badis, G., Gehrke, A. R., Talukder, S., Philippakis, A. A., Peña-Castillo, L., Alleyne, T. M., Mnaimneh, S., Botvinnik, O. B., Chan, E. T. et al. (2008). Variation in homeodomain DNA binding revealed by high-resolution analysis of sequence preferences. *Cell* **133**, 1266–1276.
- Bilioni, A., Craig, G., Hill, C. and McNeill, H. (2005). Iroquois transcription factors recognize a unique motif to mediate transcriptional repression in vivo. *Proc. Natl. Acad. Sci. USA* **102**, 14671–14676.
- Briscoe, J., Pierani, A., Jessell, T. M. and Ericson, J. (2000). A homeodomain protein code specifies progenitor cell identity and neuronal fate in the ventral neural tube. *Cell* **101**, 435–445.
- Bruneau, B. G., Bao, Z. Z., Fatkin, D., Xavier-Neto, J., Georgakopoulos, D., Maguire, C. T., Berul, C. I., Kass, D. A., Kuroski-de Bold, M. L., de Bold, A. J. et al. (2001). Cardiomyopathy in *Irx4*-deficient mice is preceded by abnormal ventricular gene expression. *Mol. Cell. Biol.* **21**, 1730–1736.
- Burmeister, M., Novak, J., Liang, M. Y., Basu, S., Ploder, L., Hawes, N. L., Vidgen, D., Hoover, F., Goldman, D., Kalins, V. I. et al. (1996). Ocular retardation mouse caused by *Chx10* homeobox null allele: impaired retinal progenitor proliferation and bipolar cell differentiation. *Nat. Genet.* **12**, 376–384.
- Cayouette, M., Barres, B. A. and Raff, M. (2003). Importance of intrinsic mechanisms in cell fate decisions in the developing rat retina. *Neuron* **40**, 897–904.
- Cheng, C. W., Chow, R. L., Lebel, M., Sakuma, R., Cheung, H. O., Thanabalasingham, V., Zhang, X., Bruneau, B. G., Birch, D. G., Hui, C. C. et al. (2005). The Iroquois homeobox gene, *Irx5*, is required for retinal cone bipolar cell development. *Dev. Biol.* **287**, 48–60.
- Chow, R. L., Snow, B., Novak, J., Looser, J., Freund, C., Vidgen, D., Ploder, L. and McInnes, R. R. (2001). *Vsx1*, a rapidly evolving paired-like homeobox gene expressed in cone bipolar cells. *Mech. Dev.* **109**, 315–322.
- Chow, R. L., Volgyi, B., Szilard, R. K., Ng, D., McKerlie, C., Bloomfield, S. A., Birch, D. G. and McInnes, R. R. (2004). Control of late off-center cone bipolar cell differentiation and visual signaling by the homeobox gene *Vsx1*. *Proc. Natl. Acad. Sci. USA* **101**, 1754–1759.
- Cohen, D. R., Cheng, C. W., Cheng, S. H. and Hui, C. C. (2000). Expression of two novel mouse Iroquois homeobox genes during neurogenesis. *Mech. Dev.* **91**, 317–321.
- Costantini, D. L., Arruda, E. P., Agarwal, P., Kim, K. H., Zhu, Y., Zhu, W., Lebel, M., Cheng, C. W., Park, C. Y., Pierce, S. A. et al. (2005). The homeodomain transcription factor *Irx5* establishes the mouse cardiac ventricular repolarization gradient. *Cell* **123**, 347–358.
- Erkman, L., Yates, P. A., McLaughlin, T., McEvilly, R. J., Whisenhunt, T., O'Connell, S. M., Krones, A. I., Kirby, M. A., Rapaport, D. H., Bermingham, J. R. et al. (2000). A POU domain transcription factor-dependent program regulates axon pathfinding in the vertebrate visual system. *Neuron* **28**, 779–792.
- Feng, L., Xie, X., Joshi, P. S., Yang, Z., Shibasaki, K., Chow, R. L. and Gan, L. (2006). Requirement for *Bhlhb5* in the specification of amacrine and cone bipolar subtypes in mouse retina. *Development* **133**, 4815–4825.
- Fode, C., Ma, Q., Casarosa, S., Ang, S. L., Anderson, D. J. and Guillemot, F. (2000). A role for neural determination genes in specifying the dorsoventral identity of telencephalic neurons. *Genes Dev.* **14**, 67–80.
- Fox, M. A. and Sanes, J. R. (2007). Synaptotagmin I and II are present in distinct subsets of central synapses. *J. Comp. Neurol.* **503**, 280–296.
- Ghosh, K. K., Bujan, S., Haverkamp, S., Feigenspan, A. and Wässle, H. (2004). Types of bipolar cells in the mouse retina. *J. Comp. Neurol.* **469**, 70–82.
- Gollisch, T. and Meister, M. (2010). Eye smarter than scientists believed: neural computations in circuits of the retina. *Neuron* **65**, 150–164.

- Gómez-Skarmeta, J. L. and Modolell, J. (2002). Iroquois genes: genomic organization and function in vertebrate neural development. *Curr. Opin. Genet. Dev.* **12**, 403-408.
- Grillenzoni, N., van Helden, J., Dambly-Chaudière, C. and Ghysen, A. (1998). The iroquois complex controls the somatotopy of *Drosophila notum* mechanosensory projections. *Development* **125**, 3563-3569.
- Guillemot, F. (2007). Cell fate specification in the mammalian telencephalon. *Prog. Neurobiol.* **83**, 37-52.
- Haverkamp, S. and Wässle, H. (2000). Immunocytochemical analysis of the mouse retina. *J. Comp. Neurol.* **424**, 1-23.
- Haverkamp, S., Ghosh, K. K., Hirano, A. A. and Wässle, H. (2003). Immunocytochemical description of five bipolar cell types of the mouse retina. *J. Comp. Neurol.* **455**, 463-476.
- Haverkamp, S., Specht, D., Majumdar, S., Zaidi, N. F., Brandstätter, J. H., Wasco, W., Wässle, H. and Tom Dieck, S. (2008). Type 4 OFF cone bipolar cells of the mouse retina express calnenilin and contact cones as well as rods. *J. Comp. Neurol.* **507**, 1087-1101.
- Jin, Z., Zhang, J., Klar, A., Chédotal, A., Rao, Y., Cepko, C. L. and Bao, Z. Z. (2003). *lrx4*-mediated regulation of *Slit1* expression contributes to the definition of early axonal paths inside the retina. *Development* **130**, 1037-1048.
- Keeley, P. W. and Reese, B. E. (2010). Role of afferents in the differentiation of bipolar cells in the mouse retina. *J. Neurosci.* **30**, 1677-1685.
- Kerschensteiner, D., Liu, H., Cheng, C. W., Demas, J., Cheng, S. H., Hui, C. C., Chow, R. L. and Wong, R. O. (2008). Genetic control of circuit function: *Vsx1* and *lrx5* transcription factors regulate contrast adaptation in the mouse retina. *J. Neurosci.* **28**, 2342-2352.
- Lebel, M., Agarwal, P., Cheng, C. W., Kabir, M. G., Chan, T. Y., Thanabalasingham, V., Zhang, X., Cohen, D. R., Husain, M., Cheng, S. H. et al. (2003). The Iroquois homeobox gene *lrx2* is not essential for normal development of the heart and midbrain-hindbrain boundary in mice. *Mol. Cell. Biol.* **23**, 8216-8225.
- Ma, Q. (2006). Transcriptional regulation of neuronal phenotype in mammals. *J. Physiol.* **575**, 379-387.
- Masland, R. H. (2001). The fundamental plan of the retina. *Nat. Neurosci.* **4**, 877-886.
- Mataruga, A., Kremmer, E. and Müller, F. (2007). Type 3a and type 3b OFF cone bipolar cells provide for the alternative rod pathway in the mouse retina. *J. Comp. Neurol.* **502**, 1123-1137.
- Matsuoka, R. L., Chivatakarn, O., Badea, T. C., Samuels, I. S., Cahill, H., Katayama, K., Kumar, S. R., Suto, F., Chédotal, A., Peachey, N. S. et al. (2011). Class 5 transmembrane semaphorins control selective Mammalian retinal lamination and function. *Neuron* **71**, 460-473.
- Milam, A. H., Dacey, D. M. and Dizhoor, A. M. (1993). Recoverin immunoreactivity in mammalian cone bipolar cells. *Vis. Neurosci.* **10**, 1-12.
- Mombaerts, P., Wang, F., Dulac, C., Chao, S. K., Nemes, A., Mendelsohn, M., Edmondson, J. and Axel, R. (1996). Visualizing an olfactory sensory map. *Cell* **87**, 675-686.
- Negishi, K., Kato, S. and Teranishi, T. (1988). Dopamine cells and rod bipolar cells contain protein kinase C-like immunoreactivity in some vertebrate retinas. *Neurosci. Lett.* **94**, 247-252.
- Ohsawa, R. and Kageyama, R. (2008). Regulation of retinal cell fate specification by multiple transcription factors. *Brain Res.* **1192**, 90-98.
- Ohtoshi, A., Wang, S. W., Maeda, H., Saszik, S. M., Frishman, L. J., Klein, W. H. and Behringer, R. R. (2004). Regulation of retinal cone bipolar cell differentiation and photopic vision by the CVC homeobox gene *Vsx1*. *Curr. Biol.* **14**, 530-536.
- Sato, M., Umetsu, D., Murakami, S., Yasugi, T. and Tabata, T. (2006). *DWnt4* regulates the dorsoventral specificity of retinal projections in the *Drosophila melanogaster* visual system. *Nat. Neurosci.* **9**, 67-75.
- Shi, Z., Trenholm, S., Zhu, M., Buddingh, S., Star, E. N., Awatramani, G. B. and Chow, R. L. (2011). *Vsx1* regulates terminal differentiation of type 7 ON bipolar cells. *J. Neurosci.* **31**, 13118-13127.
- Shi, Z., Jervis, D., Nickerson, P. E. and Chow, R. L. (2012). Requirement for the paired-like homeodomain transcription factor *Vsx1* in type 3a mouse retinal bipolar cell terminal differentiation. *J. Comp. Neurol.* **520**, 117-129.
- Shirasaki, R. and Pfaff, S. L. (2002). Transcriptional codes and the control of neuronal identity. *Annu. Rev. Neurosci.* **25**, 251-281.
- Wässle, H., Puller, C., Müller, F. and Haverkamp, S. (2009). Cone contacts, mosaics, and territories of bipolar cells in the mouse retina. *J. Neurosci.* **29**, 106-117.

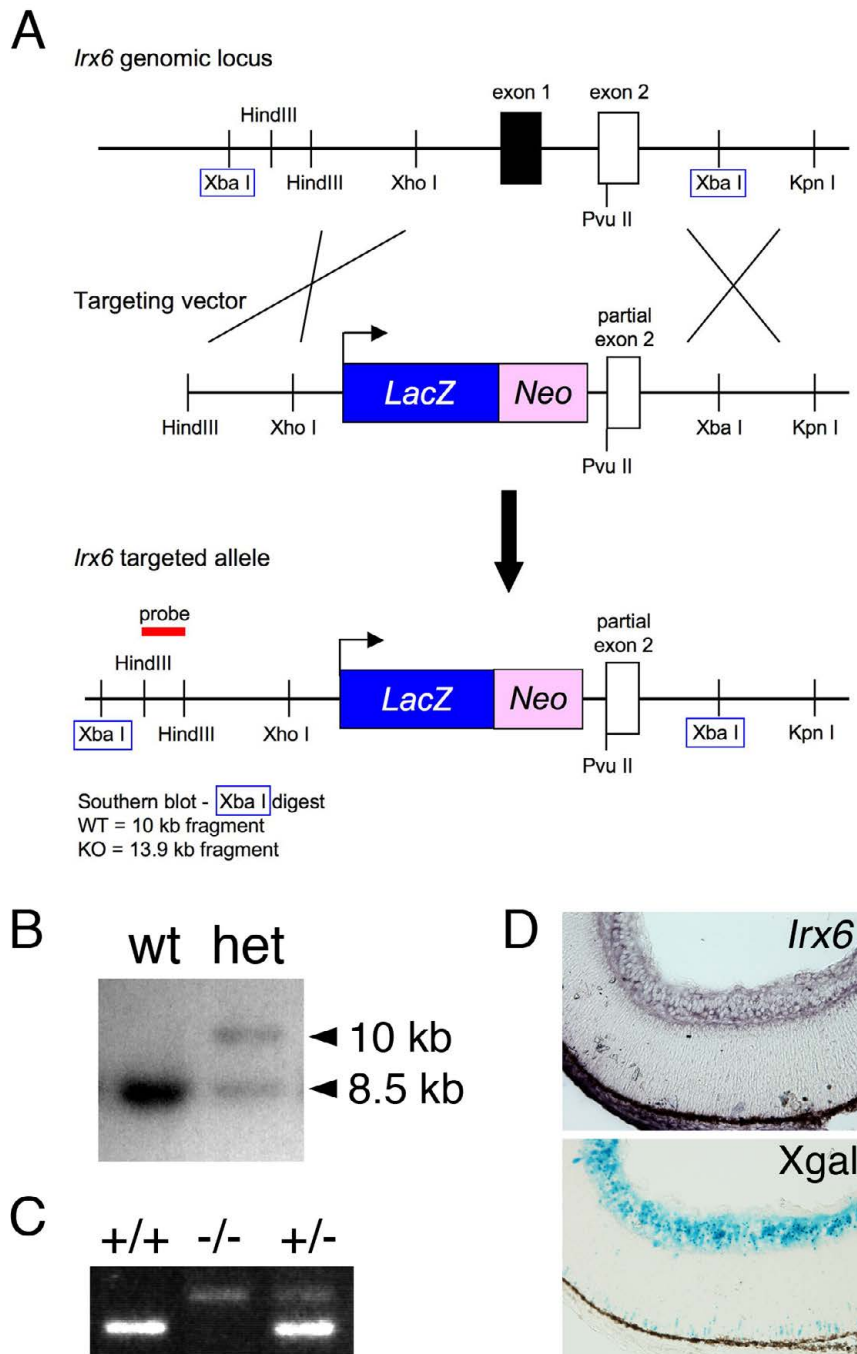


Fig. S1. Targeted disruption of *Irx6*. A 5.5 kb *NcoI/HindIII* *Irx6* fragment was cloned as the 5' arm of the targeting construct upstream of the *lacZ* gene. The targeting construct contained a neomycin resistance cassette and a thymidine kinase cassette (*Pgk-Neo-SV40 polyA*) that was cloned in reverse orientation with respect to the targeting vector. A 2 kb *PvuII/NotI* *Irx6* fragment was cloned as the 3' arm of the targeting construct. Following homologous recombination, a mutated *Irx6* allele was generated that had lost all of exon 1 and part of exon 2. (A) Construct used. (B) Southern blot of the targeted ES cell DNA, clone B3. Southern blot analysis for homologous recombinants was carried out following an *XbaI* digest using a 2 kb *HindIII* fragment probe 5' to the left arm of the targeting construct. The wild-type band size is 8.5 kb and the targeted band size is 10 kb. Two positive clones were used to give rise to the knock-in founder mice. (C) PCR showing wild-type, homozygous (*Irx6^{lacZ/lacZ}*) and heterozygous (*Irx6^{+ /lacZ}*) mice. *Irx6^{+ /lacZ}* heterozygous crosses produced offspring (+/+, +/*lacZ*, *lacZ/lacZ*) with the expected Mendelian ratio and *Irx6^{lacZ/lacZ}* mice were able to reproduce successfully. Both developing and adult *Irx6^{lacZ/lacZ}* mice were indistinguishable from their wild-type littermates in terms of size and general behavior. (D) In situ hybridization (upper) for *Irx6* expression in the P0 *Irx6^{+ /lacZ}* mouse retina and X-gal staining (lower) in an adjacent section showing the overlapping expression pattern between endogenous *Irx6* expression and expression of the *Irx6*: β gal reporter. The riboprobe corresponds to the full-length cDNA for *Irx6*. The protocol for in situ hybridization has been previously described (Chow et al., 2001), except the hybridization temperature was 56°C.

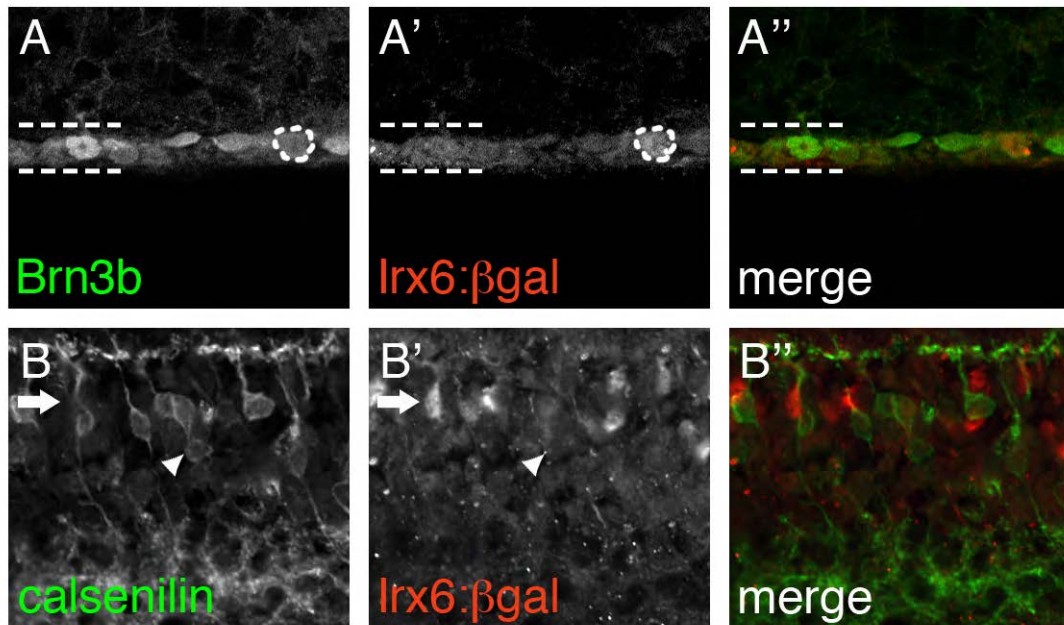


Fig. S2. The *Irx6*: β gal reporter is expressed in a subset of ganglion cells, but is not expressed in type 4 bipolar cells. (A-A'') The *Irx6*: β gal reporter co-immunolabels with the ganglion cell marker Brn3b in a subset of cells in the adult *Irx6*^{+/*lacZ*} mouse retina. The dashed lines indicate the boundary of the ganglion cell layer. The outlined cell is both positive for Brn3b and *Irx6*: β gal. **(B-B'')** In the adult *Irx6*^{+/*lacZ*} mouse retina, the type 4 bipolar cell marker calsenilin does not co-immunolabel with *Irx6*: β gal, indicating that *Irx6* is not expressed in type 4 OFF bipolar cells. The arrow indicates a cell that is positive for *Irx6*: β gal, but not for calsenilin; the arrowhead indicates a calsenilin-positive cell that is negative for *Irx6*: β gal.

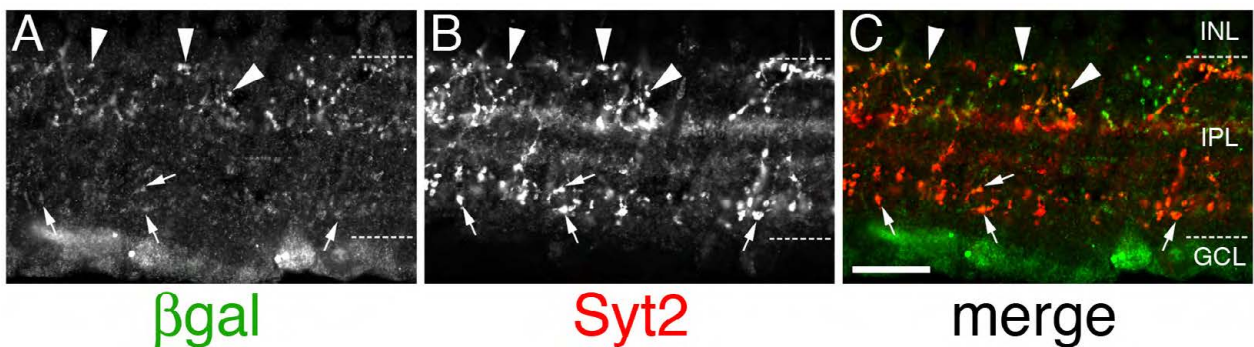


Fig. S3. *Irx6*: β gal is strongly expressed in the *Irx6*^{*lacZ*/*lacZ*} mouse and can be visualized in the inner plexiform layer. *Irx6*: β gal (A) co-immunolabels with Synaptotagmin 2 (Syt2) (B,C) in both the upper and lower zones of the inner plexiform region, corresponding to the OFF and ON projecting regions. Other ON bipolar cells (type 5 or rod bipolar cells) do not show expression of the *Irx6*: β gal reporter as all of the Cabp5-expressing cells that co-immunolabeled with *Irx6*: β gal also expressed Hcn4. Scale bar 10 μ m.

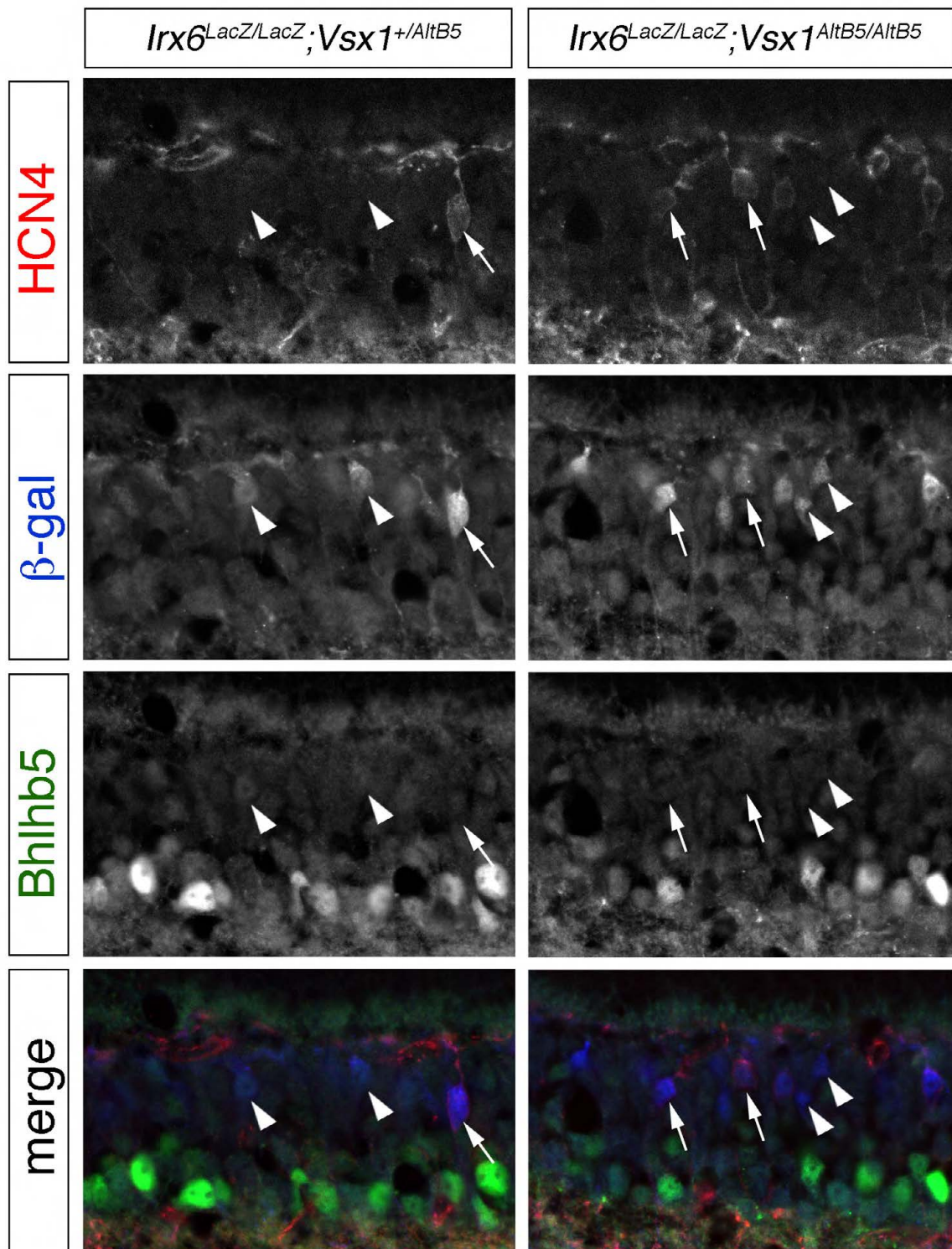


Fig. S4. In both the *Irx6*^{lacZ/lacZ}; *Vsx1*^{+/AltB5} and *Irx6*^{lacZ/lacZ}; *Vsx1*^{AltB5/AltB5} mouse, not all *Irx6*: β gal-positive cells express Hcn4. Arrowheads indicate *Irx6*: β gal-positive cells that do not express Hcn4 whereas arrows indicate *Irx6*: β gal-positive cells that express Hcn4. Bhlhb5 immunolabeling is present in some of the *Irx6*: β gal cells that do not co-immunolabel with Hcn4 in the *Irx6*^{lacZ/lacZ}; *Vsx1*^{+/AltB5} retina.

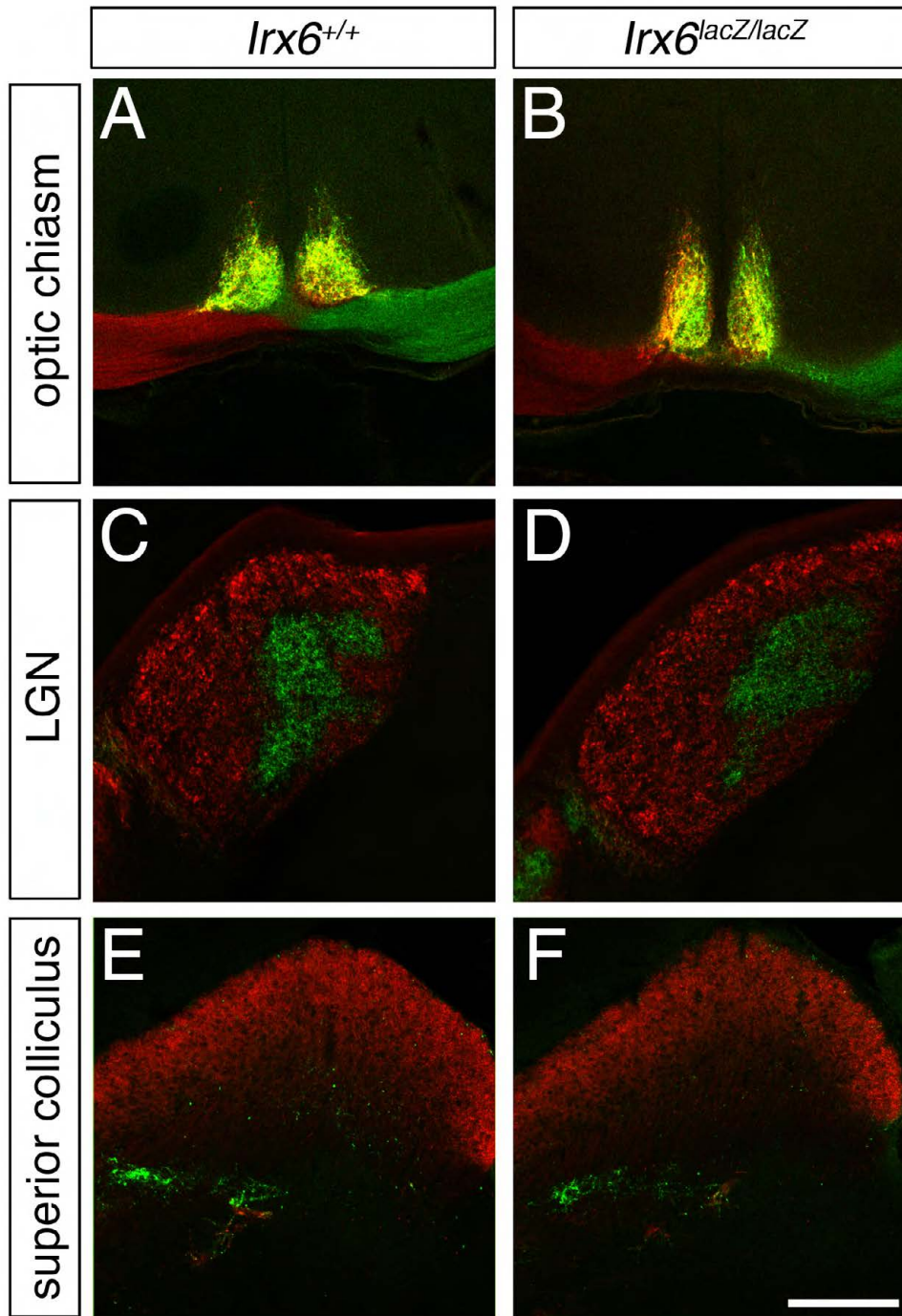


Fig. S5. Ganglion cell projections to the brain are grossly normal in *Irx6*^{lacZ/lacZ} mice. As *Irx6* is expressed in a subset of retinal ganglion cells (supplementary material Fig. S2), we investigated whether *Irx6* is required for ganglion cell axon outgrowth, migration and targeting. Cholera toxin subunit B coupled to either Alexa Fluor 488 (left eye) or Alexa Fluor 555 (right eye) (Invitrogen), was injected into the intravitreal space of the eye (2 μ l, 5 μ g/ μ l per eye) using a 33G Hamilton needle at 2 months of age. After 24 hours, mice were euthanized and brain tissue fixed for 10 minutes with 4% paraformaldehyde in phosphate-buffered saline (PBS) by trans-cardial perfusion, followed by overnight fixation of tissue in 4% paraformaldehyde in PBS at 4°C. (**A,B**) The optic nerves carrying different dyes branched out contralaterally at the optical chiasm, with a subset of nerve fibers projecting ipsilaterally with no difference between *Irx6*^{+/lacZ} (**A**) and *Irx6*^{lacZ/lacZ} (**B**) mice. (**C,D**) In the lateral geniculate nucleus, nerves projecting contralaterally (red) and ipsilaterally (green) occupy distinct regions in a manner that was indistinguishable between control *Irx6*^{+/lacZ} (**C**) and *Irx6*^{lacZ/lacZ} (**D**) mice. (**E,F**) Similarly, in the superior colliculus, where most projections were formed contralaterally, no difference was observed between control *Irx6*^{+/lacZ} (**E**) and *Irx6*^{lacZ/lacZ} (**F**) mice. Scale bar: 100 μ m in A,B,E,F; 200 μ m in C,D.

Table S1. Antibody dilutions and sources

Antigen	Antiserum	Source	Working dilution ⁵
Vsx1	Rabbit anti-Vsx1	R. L. Chow, University of Victoria, Victoria, BC	1:100
Recoverin	Rabbit anti-recoverin ¹	Millipore/Chemicon (AB5585)	1:500
NK3R	1. Rabbit anti-NK3R ²	A. Hirano, Department of Neurobiology, Los Angeles, CA	1:500
	2. Rabbit anti-NK3R ³	Calbiochem (480739)	1:5000
Cabp5	Rabbit anti-Cabp5	F. Haeseleer, Department of Ophthalmology, Seattle, WA	1:500
PKC α	Rabbit anti-PKC α	Sigma (P4334)	1:20,000
Calbindin	Mouse anti-calbindin	Sigma (C2724)	1:500
Chx10	1. Rabbit anti-Chx10	R. R. McInnes, Hospital for Sick Children, Toronto	1:500
	2. Sheep anti-Chx10	Exalpha (X1180P)	1:1000
β -Gal	1. Chicken anti- β -Gal ⁴	Abcam (ab9361)	1:300/1:12,500
	2. Rabbit anti- β -Gal	Cappel (55976), MP Biomedicals	1:5000
	3. Mouse anti- β -Gal	Sigma (G8021)	1:500
Bhlhb5	Goat anti- β 3 (E17)	Santa Cruz (sc-6045)	1:1000
HCN4	1. Guinea pig anti-HCN4 γ	F. Müller, Forschungszentrum, Jülich, Germany	1:500
	2. Rat anti-HCN4 γ PG2-1A4		1:1
Irx5	Rabbit anti-Irx5	C. C. Hui, Hospital for Sick Children, Toronto	1:50
PKA RII β	Mouse anti-PKA RII β	BD science (612550)	1:3000
Calretinin	Goat anti-calretinin	Chemicon (AB1559)	1:2500
Brn3b	Goat anti-Brn3b	Santa Cruz (sc-31989)	1:100
Syntaxin	Mouse anti-syntaxin	Sigma (S0664)	1:500
Calsenilin	Mouse anti-calsenilin	W. Wasco, Harvard Medical School, Charlestown, MA clone 40A5	1:2000
Synaptotagmin	Mouse anti-Syt2/ZNP-1	Zebrafish International Resource Center	1:250

¹Labeling for recoverin was carried out using 0.1% Triton X-100 in place of Tween 20.

²Immunolabeling for NK3R was done in the absence of horse serum.

³Mice were perfused with 4% PFA prior to enucleation and the retina was then left in 4% PFA for 20 minutes at room temperature.

⁴Chicken anti- β -gal shows some non-specific labeling of amacrine cells in this system

⁵Antibodies were diluted in PBS containing 1% horse serum and 0.1% Tween 20, except as noted above.

Table S2. Vectors used

Vector	Host	Reference to sequence number below [‡] or vector source	Putative Irx6-binding site (IBS)*
pRecoverin_1461.luc	pGL4.26 <i>KpnI</i> and <i>HindIII</i> sites	1	ACATGT
pVsx1_9130.luc	pGL3P <i>SacI</i> and <i>BglIII</i> sites	2	ACACGTGT
pVsx1_3377.luc	pGL3P <i>SacI</i> and <i>BglIII</i> sites	3	ACACGTGT
pVsx1_2232.luc	pGL3P <i>SacI</i> and <i>BglIII</i> sites	4	ACATGTGT
pNK3R_1398.luc	pGL3P <i>SacI</i> and <i>BglIII</i> sites	5	ACAGGTGT
plrx6	pBSK-EF1_ <i>SfiI</i> and <i>XbaI</i> sites	C. C. Hui, Hospital for Sick Children, Toronto	
plrx5	pBSK-EF1_ <i>SfiI</i> and <i>XbaI</i> sites	C. C. Hui, Hospital for Sick Children, Toronto	
Renilla	pRL-TK	Promega	
Luciferase with mini-promoter	pGL4.26	Promega	
Luciferase with SV40 promoter	pGL3P	Promega	

*Putative IBS identified using FIMO (<http://meme.nbcr.net/meme/intro.html>).

[‡]Appropriate restriction enzyme sites have been integrated into the primers and are found in the sequence below (primers are italicized and putative IBS is in bold).

1 . TGGTGAACAGTGCTGTGGATGTGCAAGCCAATCAAACCATTTTCCTCCTCAAGTTGC
TTTTGCTCACGGTGCTCCACGGCAGCAATAGAAACCCTAACTAACACAAGCAGAGAACT
AAGGCAGCCCATTCCTAGGCAGAAACGCAGGGGAAGATGGGAATACGTATGTAGTTCTT
GGGGATGCCTTGAAAAAGAGAAATCCCAGTGTGTAAGGTCAGTATTGTATGGAGTACCA
GGTAATAGGGTGGCATCAGAAGGAAGGGTGGGGTTTGCTTTCTAAACTTACTATACA
CCCCAACAGTCCTCTAGTCTCTAAGGAAATGGCAGGGGCAGCTATGAATAACACATAAA
CACAAACACAAAATGTATCTAAAATTACAACCCCTGAGACTACACTCAAATGACACATT
CACCATTGCCAATGTGACAGGCCCTCTGTCTCTTGCCACCTGCCTGGTCTGCCTGCTC
ACTCCTCCTAGGCAGCTTTATTCTACCTTTGTTACTTAGGAACAATAACACCAGGGCTT
AACTTATAATAGAGACTCACAAACGGACCCAGGTCCCCATGACCCAGTCTTGCCTTGAAC

ACACCATAAGTAA**ACATGT**ATAGAGCGCATCCAACACACTGAACTTTGTA~~ACTCAGGCT~~
TACCCACCTCTGTCCGCTCAGAACACTCACGTTGGACAAAATCCCGGAGAAATAATCTC
CTGTGGTTGTATAAGGCATGTTGTGGTACTGTGGTAAAGTCAAAACATTTAAACTGTGG
TAGATCAAAACATTTAGGTGAGCCTATAGTGAGTCTGGAGCCGTGTTTGTGTGTGTGTG
TGTGTGTGTTTCCAGCACCTTTTCCAGCCAGTTTGAGCTATTTTGTACTGTTCTGGCAGTG
GAGATAACAACCCACAGAACAATCTTTCCCTATCTGGCACTTCCATTCTGGCAGACA
GTTTGGGGTTTCCAGCAGCGGTGAGGAAGGAGCCATCAGAGAGTGATGGATAAAAGGT
CTTGCTGAGAAGGTGAAGTGTCTAGGCCCAAATGTGACTGGGGGAGGATTAGAAAACT
CCCATGCAGTGTAGGTTAAGTGGTAGGGCTGCCTTTAGACCCTAAGCTCCCAAACCTCT
GCACTATAAGGTCCCATGGGTGCCCTCAGATGGGGAGACAAACAGCAAGCAGTGTGGC
TCTTCGGGGGCTTAAATGCCGAGGATGCTTGGTTCAAGGGTCCCTCCTTGTTCTTTCT
TCTCAACAAGCACAGGAAAGGTAAGTGGCTGCTCTTGGCTCTTTATTTAATCTCAGAA
GGTGCCCCCTCCTCCCTCCAAGGACTGGGCAGACCTGGCCGCAAATCCCCCTAATCCA
TCAGCACCTGGGT

***a region containing more than 44% GT repeat and 20% TA repeat has been deleted from the above sequence.

2 . TACGAGCTCTTCCATAATCTGTCCATTGGTGAGAGTGGGGTGTGAAATCTCCCCT
ATTATTATGTAATGTTCAATGTGTGTTTTGAGCTTTAGTAATGTTTCTTTT**ACACGTGT**
GGGTGCCCTTGCCATGGGGCATAACATGTTTAGAATTGAGAATCAATTTGGATTTTTC
GTATGGTGGGTATGAATAAGATTTCCCATCTCTTTTGATAACTTTTGGTTGAAAGTCTA
TTTTACTGGATATTAGAATGGCTACTTCAGCTTGTCTTAGATCTGTT

3 . TACGAGCTCAGTACTTGACGATGAGGTCCCTGGACACAAAGCTGGAGTCAGTGTCTG
AGTATAGATTATGAGGGGTCGGATCTCAGAACAGAGGGATAGCAGAGAAGCAGGAGA
AGGAGCCACGCAAAGTTGCCACTGCCCTATCCACGAATGGGGAGGAACTGGAAACAGAC
ACTGCAATGTCTCCTTCAA**ACACGTGT**GTGACCTCTTAGTAACTCAGTGTGAGACT
CTGTTTTGTGGTTTTCTGTCTACGGAAGAACAATTGCCCCATCGAGGCAGGGTAAAA
AGCCAGTCCATATTTATCTAGTACAAGGGTCCAAGAACGGAGTCTGAGTGGGACACCAA
CAACCTGGGAAGGAGAAAGCAATGTGGAACGAGATCTGCGATCTG

4 . TACGAGCTCCGAATCTGATAATAGTTTGGCTTTTAGCTTTTCTTACCCTGAGATTTT
TTGATATGTTGAATATGGGTAGATAACCTCACAGTTGAATGGTATTGTTTTT**ACACGTGT**
TTTATAACTACTGAG**ACATGTGT**GTGATGGGTGCACAAGCTTCCCTGGGCTATGTCTCT
AGGATTCGTGCATCAGGGCAGGGTGGAGTTTGGACAAAGATTTGATGTCACAAATCCTGC
CTTAGATCTGTT

5 . TACGAGCTCCAACAGGCAGTAATGATCACATATTTATTTGATAAAAAAAAAATGTGTC
TTTTTGAAATGCATTCTGCCTAATAGCATTGATTTCTTTTCCACTTTGTAATAACTC
CACCAAAATCGTGGATGTGACAT**ACAGGTGT**TAGTTTTCTACTGACATGTGGTACTTA
CTACATTATTAGCAATTCCTGAAAGCCTGTTTTGTTGCCTGAAAGACCACTTCTCTATC
GTCATCGCCACCTTGATAACCCAGATCCCAAGTGAAAGGTATAATTACTTCTTCTACCGA
TCTGAATATCGTTATCTAGATCTGTT